Lithos 196–197 (2014) 213–231

Contents lists available at ScienceDirect

Lithos

journal homepage: www.elsevier.com/locate/lithos

Transition from oceanic to continental lithosphere subduction in southern Tibet: Evidence from the Late Cretaceous–Early Oligocene (~91–30 Ma) intrusive rocks in the Chanang–Zedong area, southern Gangdese

Zi-Qi Jiang [a,b], Qiang Wang [a,*], Derek A. Wyman [c], Zheng-Xiang Li [d], Jin-Hui Yang [e], Xiao-Bing Shi [b], Lin Ma [a], Gong-Jian Tang [a], Guo-Ning Gou [a], Xiao-Hui Jia [a], Hai-Feng Guo [a]

[a] State Key Laboratory of Isotope Geochemistry, Guangzhou Institute of Geochemistry, Chinese Academy of Sciences, Guangzhou 510640, China
[b] Key Laboratory of Marginal Sea Geology, South China Sea Institute of Oceanology, Chinese Academy of Sciences, Guangzhou 510301, China
[c] School of Geosciences, The University of Sydney, NSW 2006, Australia
[d] ARC Centre of Excellence for Core to Crust Fluid Systems (CCFS) and the Institute for Geoscience Research (TIGeR), Department of Applied Geology, Curtin University, GPO Box U1987, Perth, WA 6845, Australia
[e] State Key Laboratory of Lithospheric Evolution, Institute of Geology and Geophysics, Chinese Academy of Sciences, Beijing 100029, China

ARTICLE INFO

Article history:
Received 5 October 2013
Accepted 3 March 2014
Available online 12 March 2014

Keywords:
Adakites
Oceanic subduction
Continental collision
Slab breakoff
Continental subduction
Southern Tibet

ABSTRACT

Little is known about the detailed processes associated with the transition from oceanic to continental lithosphere subduction in the Gangdese Belt of southern Tibet (GBST). Here, we report zircon U–Pb age, major and trace element and Sr–Nd–Hf isotopic data for Late Cretaceous–Early Oligocene (~91–30 Ma) intermediate-acid intrusive rocks in the Chanang–Zedong area immediately north of the Yarlung–Tsangpo suture zone. These rocks represent five magmatic episodes at ~91, ~77, ~62, ~48, and ~30 Ma, respectively. The 91–48 Ma rocks have slightly lower initial $^{87}Sr/^{86}Sr$ (0.7037 to 0.7047), and higher $\varepsilon_{Nd}(t)$ (+1.8 to +4.3) and $\varepsilon_{Hf}(t)$ (+3.5 to +14.7) values in comparison with those (0.7057 to 0.7062, −3.3 to −2.5 and +2.2 to +6.6) of the ~30 Ma intrusive rocks. The ~91, ~62 and ~30 Ma rocks are geochemically similar to slab-derived adakites. The ~91 Ma Somka adakitic granodiorites were likely derived by partial melting of the subducting Neo-Tethyan oceanic crust with minor oceanic sediments, and the ~91 Ma Somka dioritic rocks with a geochemical affinity of adakitic magnesian andesites likely resulted from interactions between adakitic magmas and overlying mantle wedge peridotite. The ~77 Ma Luomu diorites were probably generated by partial melting of juvenile basaltic lower crust. The ~62 Ma Naika and Zedong adakitic diorites and granodiorites were likely generated mainly by partial melting of thickened juvenile mafic lower crust but the source region of the Zedong adakitic rocks also contained enriched components corresponding to Indian continental crust. The ~48 Ma Lamda granites were possibly generated by melting of a juvenile basaltic crust. The younger (~30 Ma) Chongmuda adakitic quartz monzonites and minor granodiorites were most probably derived by partial melting of Early Oligocene northward-subducted Indian lower crust beneath the southern Lhasa Block. Taking into account the regional tectonic and magmatic data, we suggest that the Gangdese Belt of southern Tibet (GBST) underwent a tectonodynamic transition from oceanic subduction to continental subduction between 100 and 30 Ma. It evolved through four stages: 100–65 Ma roll-back of subducted Neo-Tethyan oceanic lithosphere; 65–60 Ma initial collision between Indian and Asian continents; 60–40 Ma breakoff of subducted Neo-Tethyan oceanic lithosphere; and ~30 Ma northward subduction of the Indian continent.

1. Introduction

Collisional orogens can undergo three major stages: subduction of oceanic lithosphere, continental collision, and continental subduction (e.g., Chung et al., 2005). However, it is often difficult to identify the processes associated with the transition from oceanic to continental subduction during the evolution of such an orogen. The Tibetan Plateau, a result of the largest active collisional orogen on Earth, is an outstanding natural laboratory in which to study such processes (Chung et al., 2005; Yin and Harrison, 2000).

The Gangdese Belt on the southernmost margin of the Asian continent contains voluminous Jurassic–Miocene magmatic rocks (Fig. 1a). In recent years, these magmatic rocks have been used extensively to

* Corresponding author.
E-mail address: wqiang@gig.ac.cn (Q. Wang).

http://dx.doi.org/10.1016/j.lithos.2014.03.001
0024-4937/

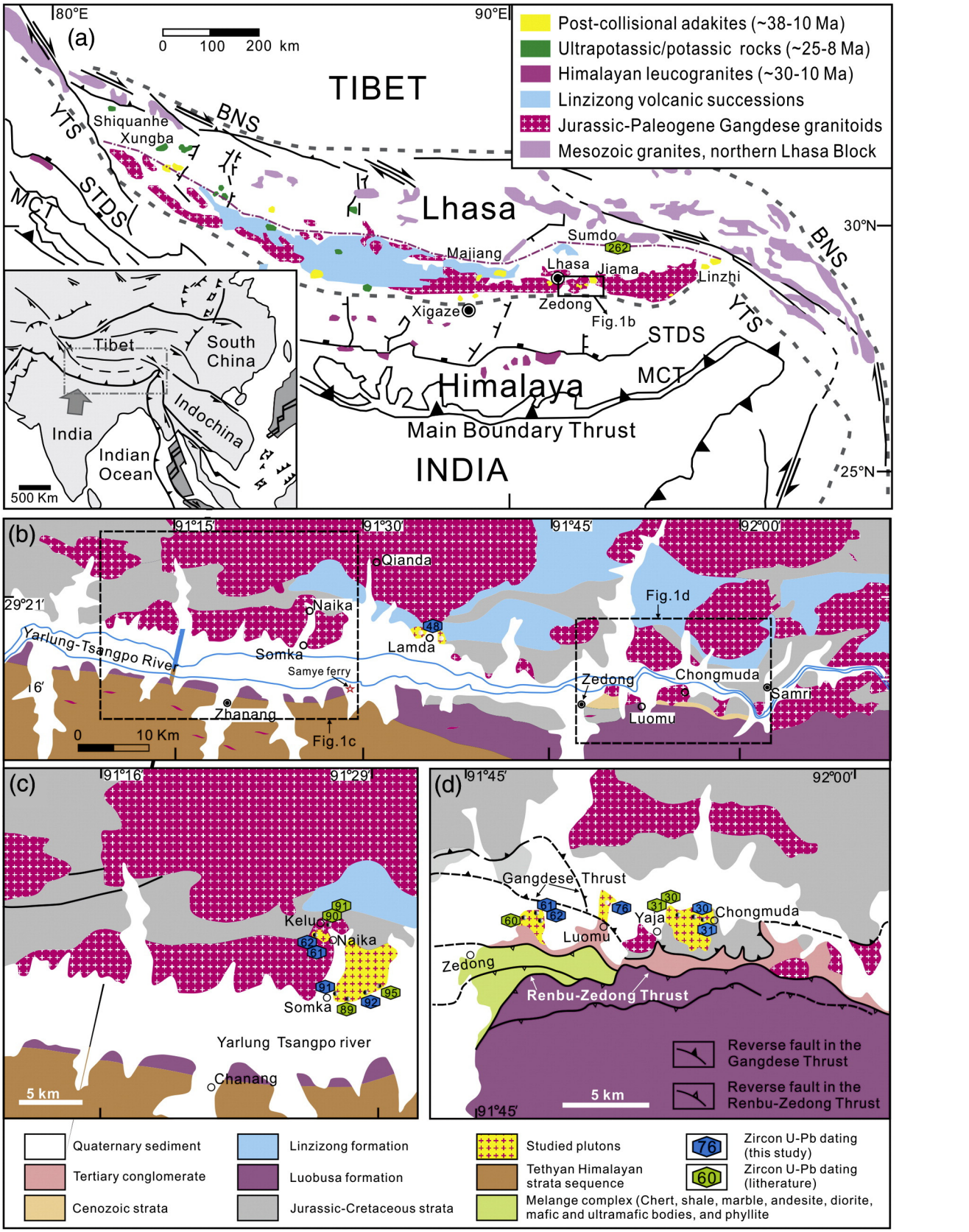

Fig. 1. (a) Map of southern Tibetan Plateau showing major blocks and temporal–spatial distribution of Cenozoic magmatic rocks (modified from Chung et al., 2009). BNS: Bangong–Nujiang suture; YTS: Yarlung–Tsangpo suture; MCT: Main Central Thrust; STDS: South Tibet Detachment System. The Zircon SHRIMP U–Pb age data (~262 Ma) of the Sumdo eclogites are from Yang et al. (2009). (b) Simplified geologic map showing the outcrops of the magmatic rocks in the Chanang–Zedong area, southern Gangdese belt. (c) Simplified geologic map of the Zhanang area. (d) Simplified geologic map of the Zedong area (modified from Harrison et al., 2000). Zircon U–Pb data are from these references (Chung et al., 2009; Harrison et al., 2000; Jiang et al, 2012; Wen et al, 2008b).

trace the geotectonic evolution of southern Tibet because they are closely related to the prolonged subduction of the Neo-Tethyan oceanic lithosphere, the subsequent collision between the Indian and Asian continents and subduction of the India continental lithosphere (e.g., Chu et al., 2011; Chung et al., 2005, 2009; Ji et al., 2009a,b; Jiang et al., 2011, 2012; Ma et al., 2013a,b,c; Wen et al., 2008a,b).

Details about the transition from Neo-Tethyan oceanic slab subduction to Indian continental subduction remain unclear. For instance, the age of the initial India–Asia continent collision is still much debated. This age is commonly considered to correspond to the closure of the Neo-Tethys ocean basin and the first contact between the Indian and Asian continents (e.g., Ding et al., 2005). However, the estimated timing for the initial collision ranges from 70 to 25 Ma (Aitchison et al., 2007; Cai et al., 2011; Chu et al., 2011; Ding et al., 2005; Hu et al., 2012; Lee and Lawver, 1995; Mo et al., 2007; Najman et al., 2010; Sun et al., 2012; van Hinsbergen et al., 2012; Yi et al., 2011). Continental subduction may have occurred following the initial collision, and would cause crustal thickening. For example, geophysical data and tectonic studies demonstrate that northward subduction of the Indian continent presently extends beneath the Bangong–Nujiang suture in central Tibet (Nabelek et al., 2009; Tapponnier et al., 2001; Yin and Harrison, 2000; Zhao et al., 2010). Owing to the uncertainties about the timing of initial collision, however, the age of continental subduction initiation is also disputed (Chu et al., 2011; Chung et al., 2009; Jiang et al., 2011; Kapp et al., 2007; Tapponnier et al., 2001).

Adakitic rocks, which have intermediate to felsic compositions combined with high Sr/Y and La/Yb ratios (Castillo, 2012; Defant and Drummond, 1990), have been widely used for tracing various geodynamic processes (e.g., melting of subducting oceanic or continental crust, or thickened crust) (Chung et al., 2003; Hou et al., 2004; Jiang et al., 2012; Wang et al., 2008b). Experimental studies suggest that adakitic magmas are generally derived by partial melting of basaltic rocks with garnet as a major residual phase in their source, but with little or no plagioclase, indicating that they are generated at high pressures of 1.2–1.5 GPa and depths of >40–50 km (Rapp et al., 1999; Sen and Dunn, 1994; Xiong et al., 2005).

In the Chanang–Zedong region, immediately north of the Yarlung–Tsangpo Suture zone, there are abundant Late Cretaceous–Early Cenozoic magmatic rocks (Fig. 1b), which provide excellent opportunities for tracing in detail the processes associated with the transition from oceanic subduction to continental collision and continental subduction. In this study, we present geochronological results, combined with major and trace element geochemical and Sr–Nd–Hf isotopic data for Late Cretaceous–Early Oligocene (91–30 Ma) intrusive rocks in the Chanang–Zedong area in order to unravel these processes.

2. Geological background

The Tibetan Plateau mainly consists of four east–west trending continental blocks. From north to south, they are the Songpan–Ganze, Qiangtang, Lhasa and Himalaya blocks, separated by the Jinsha, Bangong–Nujiang and Yarlung–Tsangpo suture zones, respectively (Yin and Harrison, 2000). The Lhasa Block in southern Tibet is bounded by the Bangong–Nujiang suture (BNS) to the north and the Yarlung–Tsangpo suture (YTS) to the south (Fig. 1a) (Yin and Harrison, 2000). The Lhasa Block can be subdivided into the northern, central, and southern subterranes or blocks, separated by the Shiquan River–Nam Tso Mélange Zone and Luobadui–Milashan Fault (Zhu et al., 2013). With the exception of the Amdo microcontinent with Cambrian or Neoproterozoic crystalline basement (e.g., Guynn et al., 2012), the northern Lhasa subterrane mainly consists of a juvenile crust covered by Middle Triassic–Cretaceous sedimentary rocks with early Cretaceous volcanic rocks and associated granitoids (Zhu et al., 2011; Zhang et al., 2013, 2014). The Precambrian basement in the central Lhasa subterrane is represented by a part of the Nyainqêntanglha Group (Dong et al., 2011; Zhu et al., 2013), covered by Cambrian to Premain metasedimentary and Upper Jurassic–Lower Cretaceous sedimentary units with abundant volcanic rocks (Zhang et al., 2013, 2014; Zhu et al., 2013). A part of the Nyingchi Group in the eastern southern Lhasa subterrane contains Precambrian metamorphic rocks (Zhang et al., 2014; Zhu et al., 2013).

The Gangdese Belt, located at the southern margin of the Lhasa Block (Fig. 1a), is dominated by the Gangdese batholith (Ji et al., 2009b; Wen et al., 2008b). The batholith was mainly emplaced from the Late Triassic to the Eocene (205–40 Ma) with two age peaks at 100–80 and 65–40 Ma (Ji et al., 2009b; Ma et al., 2013a; Wen et al., 2008b). Mesozoic volcanic rocks include the Lower Jurassic Yeba Formation (190–174 Ma) and the Upper Jurassic–Lower Cretaceous Sangri Group (Zhu et al., 2013). The Linzizong volcanic rocks (69–43 Ma) are widely distributed in southern Tibet and consist of calc-alkaline andesitic flows, tuffs and breccias, and dacitic to rhyolitic ignimbrites (e.g., Lee et al., 2012). After a ~10 Ma (i.e., 40–30 Ma) period of quiescence, a renewal of magmatic activity occurred between 30 Ma and 8 Ma (Chung et al., 2009; Hou et al., 2004; Zhao et al., 2009). This renewed magmatic pulse in the Gangdese Belt is mainly represented by post-collisional adakitic and potassic–ultrapotassic rocks located close to N–S trending normal faults, rifts, or grabens (Fig. 1a).

The Chanang–Zedong area in the southern Gangdese batholith belt is adjacent to the Yarlung–Tsangpo suture (Fig. 1a). Intrusive rocks in the Chanang–Zedong area were mainly generated during the Jurassic–Oligocene (157–30 Ma) (Aitchison et al., 2000; Harrison et al., 2000; McDermid et al., 2002; Wen et al., 2008b). Investigations along the Yarlung–Tsangpo suture reveal that the Zedong area, termed the "Zedong terrane" (Aitchison et al., 2000), represents fragmented remnants of an intra-oceanic island arc, which developed with the opening and closing of a Neo-Tethys ocean during the Late Jurassic–Early Cretaceous (Aitchison et al., 2000; McDermid et al., 2002). This fragmented unit crops out over approximately 25 km^2 near Zedong township, extending at least as far west as the Samye Ferry area and eastward to near the Luomu area (Fig. 1b). It is in tectonic contact with ophiolitic rocks to its south and the southern Gangdese arc to its north (Aitchison et al., 2000) (Fig. 1b). It contains some Late Jurassic igneous and volcaniclastic rocks including basaltic–andesitic pillow lavas, breccias, tuffs, flows, cherty tuffs, dacites, rhyolites, gabbros, diorites and quartz diorites (McDermid et al., 2002).

Six plutons in the Chanang–Zedong area were investigated in this study (Fig. 1b). The Naika, Somka and Lamda plutons are located on the north side of Yarlung Tsangpo River (Fig. 1b and c) where they intrude Jurassic strata. The Somka pluton has zircon U–Pb ages ranging from 95.0 to 89.3 Ma (Wen et al., 2008b). The Zedong, Luomu and Chongmuda plutons are located south of the Yarlung Tsangpo River (Fig. 1b), intrude Jurassic sediments and Cretaceous volcaniclastics and are overlain by Quaternary sediments (Fig. 1d). The Zedong granodiorites have biotite/hornblende $^{40}Ar/^{39}Ar$ and zircon U–Pb ages of 52.6–63.0 Ma (Harrison et al., 2000; Wen et al., 2008b). The Chongmuda granodiorites have zircon U–Pb and $^{40}Ar/^{39}Ar$ biotite/hornblende ages of ~30 Ma (Chung et al., 2009; Hou et al., 2012; Jiang et al., 2011) and 27.8–33.2 Ma (Harrison et al., 2000), respectively.

3. Rock types and petrography

We collected 48 samples from the Somka, Naika, Lamda, Zedong, Luomu and Chongmuda plutons (see Fig. 1b and c for sample locations). The six plutons show similar rock assemblages. Sample names, localities, coordinates, and petrographic characteristics of the intrusive rock samples are listed in Appendix 1. Field geological characteristics, photomicrographs and detailed petrographic characteristics of the intrusive rocks and associated enclaves are shown in Appendices 2 and 3.

The Somka pluton is composed of granodiorites plus minor granites and mafic dioritic rocks. The Naika pluton consists of mafic enclave-bearing diorites. The Lamda pluton comprises diorites and granodiorites. The Zedong pluton comprises granodiorites, minor

granites and dioritic enclaves. The Luomu pluton consists mainly of diorites. The Chongmuda pluton comprises quartz monzonites, minor granodiorites and dioritic enclaves (Jiang et al., 2011).

4. Analytical results

Analytical methods used for the determination of whole-rock major and trace element abundances and Sr–Nd isotope compositions, zircon U–Pb ages and Lu–Hf isotope compositions are presented in Appendix 4, and related analytical data of studied samples with international reference samples and replicate samples are listed in Appendices 5–9.

4.1. Zircon geochronology

Cathodoluminescence (CL) images of all zircon grains used for SHRIMP and LA-ICP-MS U–Pb dating show that these zircon grains contain micro-scale oscillatory zoning (Fig. 2). Moreover, they also have high Th/U ratios (0.12–2.60), suggesting a magmatic origin (Belousova

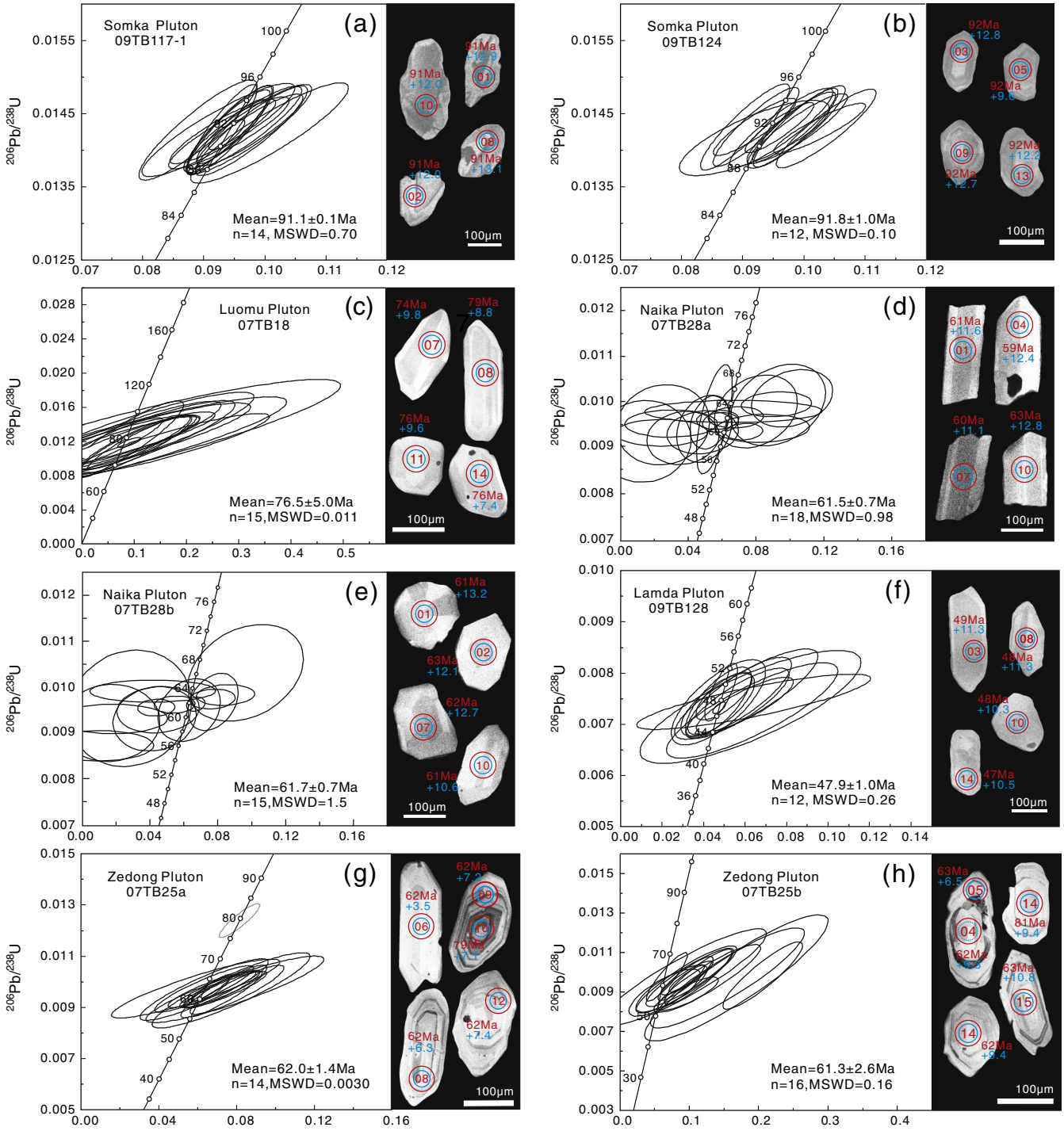

Fig. 2. LA-ICP-MS (a–c and f–h) and SHRIMP (d–e) zircon U–Pb concordia diagrams and cathodoluminescence images: (a) the Somka diorite; (b) the Somka granite; (c) the Luomu diorite; (d) the Naika diorite; (e) the Naika mafic enclave; (f) the Lamda granodiorite; (g) the Zedong granodiorite; and (h) the Zedong mafic enclave. Red and blue circles indicate the locations of LA-ICP-MS or SHRIMP U–Pb age and LA-MC-ICP-MS Hf analyzing spots, respectively. The U–Pb ages and $\varepsilon_{Hf}(t)$ values are given for each spots. (For interpretation of the references to color in this figure legend, the reader is referred to the web version of this article.)

et al., 2002). U–Pb concordia diagrams of analyzed zircons are shown in Fig. 2 and detailed geochronological descriptions are put in Appendix 10.

The Somka and Luomu intrusive rocks were generated in the Late Cretaceous with ages of ~90 Ma and 77 Ma, respectively (Fig. 2a–c), and the former was contemporary with the Kelu adakitic intrusive rocks (~90 Ma) (Jiang et al., 2012) near Somka (Fig. 1c). The Naika, Zedong, Lamda and Chongmuda intrusive rocks were generated in the Paleogene. The host rocks and enclaves for both the Naika and Zedong plutons were contemporary and generated at ~62 Ma (Fig. 2d–e and g–h). The Lamda intrusive rocks were produced at ~48 Ma (Fig. 2f). Host rocks and enclaves for the Chongmuda pluton were also contemporaneous and generated at ~30 Ma (Jiang et al., 2011).

4.2. Major and trace elements

4.2.1. The Somka intrusive rocks

The Somka samples plot in the fields of granites, granodiorites and diorites on SiO_2 vs. $Na_2O + K_2O$ diagrams (Fig. 3a). The granodiorites are high-K calc-alkaline and metaluminous rocks, and the granite sample is high-K calc-alkaline and weakly peraluminous (Fig. 3b–c). They are characterized by high SiO_2, K_2O and K_2O/Na_2O values, and low MgO, $Mg^{\#}$ ($100 \times Mg / (Mg + Fe^{total})$), Cr and Ni values (Fig. 3;

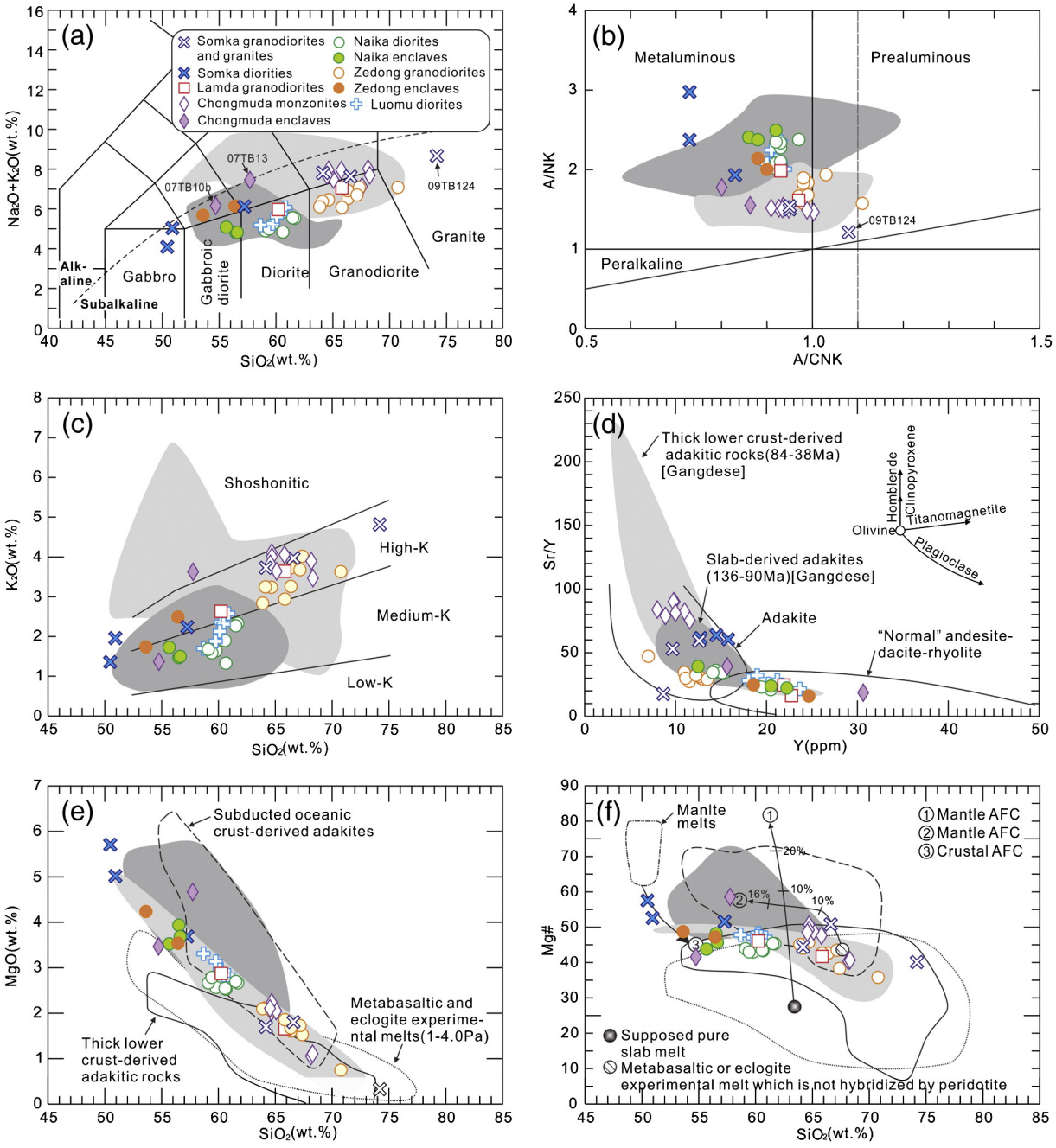

Fig. 3. (a) SiO_2 versus $Na_2O + K_2O$ diagram (Middlemost, 1994). (b) A/NK ($Al_2O_3 / (Na_2O + K_2O)$) versus A/CNK ($Al_2O_3 / (CaO + Na_2O + K_2O)$) diagram. (c) SiO_2 versus K_2O diagram (Peccerillo and Taylor, 1976). (d) Y versus Sr/Y diagram (Defant et al., 1993). Crystal fractionation paths of the primary minerals are from Castillo et al. (1999). (e) SiO_2 versus MgO diagram (Wang et al., 2006b). (f) SiO_2 versus $Mg^{\#}$ ($100 \times Mg^{2+} / (Fe^{2+} + Mg^{2+})$) diagram (Wang et al., 2006b). The data for the 84–38 Ma adakites in southern Tibet are from Guan et al. (2012), Ji et al. (2012) and Wen et al. (2008a). The data for the 136–90 Ma adakites in southern Tibet are from Jiang et al. (2012), Ma et al. (2013c), Zhang et al. (2010a) and Zhu et al. (2009). The data for the ~30 Ma adakites of the Chongmuda Plutons in southern Tibet are from Jiang et al. (2011).

Appendix 8). In contrast, the diorites have distinctly lower SiO_2 and K_2O/Na_2O values, and high MgO, $Mg^{\#}$ values (Fig. 3e and f), which are similar to magnesian andesites in arc settings (e.g., Escuder et al., 2007).

The Somka granodiorites and diorites display low concentrations of heavy rare earth elements (HREEs) and Y but high Sr contents with high Sr/Y and La/Yb ratios, indicating that they have adakitic affinities (Fig. 3d) (Defant and Drummond, 1990). The granodiorites and diorites show light rare earth element (LREE) enrichment and HREE depletion with negligible to positive Eu anomalies whereas the granite sample is characterized by a distinct depletion of the middle REEs (MREEs) and negative Eu anomalies (Fig. 5a). All of these rocks are characterized by enrichment of large ion lithophile elements (LILEs) and relative depletion of high field strength elements (HFSEs) (Fig. 5b). Compared to granodiorites and diorites, the granite sample exhibits strong negative P and Ti anomalies.

4.2.2. The Luomu intrusive rocks

The Luomu samples plot in the field of diorites (Fig. 3a) with $Mg^{\#}$ values of 47–48 (Appendix 8). They are medium-K calc-alkaline and metaluminous (Fig. 3b and c) and have enriched LREE but almost flat HREE patterns, slightly negative Eu anomalies (Fig. 5c) and significant Nb–Ta–Zr–Hf–Ti depletion (Fig. 5d).

4.2.3. The Zedong and Naika intrusive rocks

Samples of the Zedong and Naika intrusive rocks plot in the fields of diorites, granodiorites and granites (Fig. 3a). They have low $Mg^{\#}$ values (Fig. 3) and are medium- and high-K calc-alkaline, most are metaluminous (Fig. 3b and c). The mafic enclaves from the Zedong and Naika intrusive rocks are slightly lower in SiO_2 and higher in MgO and $Fe_2O_3^T$ contents relative to their host rocks (Appendix 8, Fig. 3).

The Zedong granodiorites exhibit LREE enrichment, HREE, Nb and Ti depletion, negligible Eu anomalies, and positive Sr anomalies (Fig. 5e and f). They are slightly depleted in MREEs relative to HREEs, indicating that amphibole was a possible residual phase in the source region. The Naika diorites also exhibit LREE enrichments, HREE, Nb and Ti depletion, and positive Sr anomalies, similar to those of the Zedong granodiorites (Fig. 5g and h). The Zedong and Naika intrusive rock samples plot in the field of adakites due to their relatively high Sr, Sr/Y and La/Yb values, and low Y and Yb contents (Appendix 8, Fig. 3d).

The Zedong mafic enclaves show geochemical features similar to those of the host rocks, e.g., slightly negative or positive Eu anomalies (Fig. 5e). Compared to the granodiorites, the Zedong dioritic enclaves have lower Th and U contents (Fig. 5f). They exhibit REE and trace element patterns similar to those of the Naika host rocks, e.g., LREE enrichment and HREE depletion, negligible Eu and positive Sr anomalies, and Nb and Ta depletion (Fig. 5g and h). However, the enclaves have higher Th and U contents than the Naika diorites.

4.2.4. The Lamda pluton

The Lamda pluton samples plot in the fields of granodiorite and diorite. They are metaluminous and high-K calc-alkaline (Appendix 8, Fig. 3) and show enriched LREE and slightly flat HREE patterns with slightly negative Eu anomalies (Fig. 5i) and Nb–Ta–Ti depletions (Fig. 5j).

4.2.5. The Chongmuda pluton

The Chongmuda intrusive rocks consist of quartz monzonites and minor granodiorites and mafic microgranular enclaves. The host rocks are high-K calc-alkaline (Fig. 3c), mostly metaluminous (Fig. 3b) and geochemically similar to adakites (Appendix 8, Fig. 3d) (Jiang et al., 2011). They also have slightly negative Eu anomalies, Nb–Ta–Ti depletions (Fig. 5k and l), low MgO and $Mg^{\#}$ (41–51) values and variable K_2O contents with K_2O/Na_2O ratios. The mafic microgranular enclaves can be subdivided into low silica–Nb rich and high silica–high magnesian subtypes (Appendix 8) (Jiang et al., 2011). The low silica–Nb rich subtype sample (07TB10b) has lower SiO_2, MgO and $Mg^{\#}$ values with high Nb, Nb/La (0.68) and Nb/U values, geochemically similar to those of Nb-enriched basaltic rocks (e.g., Wang et al., 2008a). The high silica–high magnesian subtype sample (07TB13) has higher SiO_2 and MgO, $Mg^{\#}$ values, Ni, and Cr compared to sample 07TB10b and is geochemically similar to typical magnesian andesites (e.g., Escuder et al., 2007). They have low Yb and Y contents, high Al_2O_3 contents and obvious Nb and Ta anomalies, similar to those of the Chongmuda host rocks (Jiang et al., 2011).

4.3. Sr–Nd–Hf isotope compositions

The Late Cretaceous (91–77 Ma) Somka and Luomu intrusive rocks have similar Sr–Nd–Hf isotopic compositions. The Somka intrusive rocks have relatively homogeneous $(^{87}Sr/^{86}Sr)_i$ ratios and $\varepsilon_{Nd}(t)$ values (Appendix 8, Fig. 6a) with relatively homogeneous zircon $\varepsilon_{Hf}(t)$ values (Appendix 9, Fig. 7a and b). The Luomu diorites also have homogeneous $(^{87}Sr/^{86}Sr)_i$ ratios and $\varepsilon_{Nd}(t)$ values (Fig. 6a) with slightly variable zircon $\varepsilon_{Hf}(t)$ values (Fig. 7c).

The Early Cenozoic (~62 Ma) Zedong and Naika plutons have slightly different Nd–Sr–Hf isotope compositions. The Zedong intrusive rocks have higher $(^{87}Sr/^{86}Sr)_i$ and lower $\varepsilon_{Nd}(t)$ and zircon $\varepsilon_{Hf}(t)$ than those of the Naika intrusive rocks, respectively (Figs. 6a and 7d and g). Mafic enclaves from the Zedong pluton also have higher $(^{87}Sr/^{86}Sr)_i$ (0.7047), and lower $\varepsilon_{Nd}(t)$ (+1.7) and zircon $\varepsilon_{Hf}(t)$ (+6.4 to +13.4) than respective compositions of mafic enclaves from the Naika pluton (Figs. 6a and 7e and h).

The Eocene (~48 Ma) Lamda granites have homogeneous whole rock $(^{87}Sr/^{86}Sr)_i$ ratios and $\varepsilon_{Nd}(t)$ (Fig. 6a) with zircon $\varepsilon_{Hf}(t)$ values ranging from +9.7 to +12.0 (Fig. 7f). The Oligocene (~30 Ma) Chongmuda intrusive rocks have more variable and higher $(^{87}Sr/^{86}Sr)_i$, negative $\varepsilon_{Nd}(t)$ and lower zircon $\varepsilon_{Hf}(t)$ values (Appendix 8–9, Fig. 6a and c) (Jiang et al., 2011). Two types of mafic enclaves from the Chongmuda pluton have similar $(^{87}Sr/^{86}Sr)_i$ but more variable $\varepsilon_{Nd}(t)$ (Fig. 6a) and zircon $\varepsilon_{Hf}(t)$ values (+0.7 to +6.9) (Fig. 7i and j) (Jiang et al., 2011).

5. Petrogenesis

5.1. Adakitic rocks and associated rocks

Except for the ~77 Ma Luomu and ~48 Ma Lamda intrusions, most other intrusive rocks in the Chanang–Zedong area (e.g., Somka, Zedong, Naika and Chongmuda) have affinities with adakitic rocks (Fig. 3d). In general, adakitic rocks may be generated by various different processes: (a) melting of subducted young and hot oceanic crust (Mechanism A: Defant and Drummond, 1990); (b) partial melting of delaminated lower crust (Mechanism B: Wang et al., 2006a, b); (c) partial melting of subducted continental crust (Mechanism C: Jiang et al., 2011; Wang et al., 2008b); (d) partial melting of thickened basaltic lower crust (Mechanism D: Chung et al., 2003; Hou et al., 2004; Wang et al., 2005); (e) assimilation and fractional crystallization (AFC) or fractional crystallization from parental basaltic magmas (Mechanism E: Castillo et al., 1999; Castillo, 2012; Macpherson et al., 2006); and (f) magma mixing between felsic and basaltic magmas (Mechanism F: Guo et al., 2007b; Streck et al., 2007). The petrogenesis of multiple generations of adakitic rocks in the Chanang–Zedong area is discussed in relation to these mechanisms.

5.1.1. ~91 Ma

5.1.1.1. Mechanisms B–F. The geochemical characteristics of the Somka adakitic granodiorites and magnesian diorites are inconsistent with partial melting of delaminated or subducting continental lower crust (Mechanism B–C). Adakitic rocks derived by these processes usually exhibit distinctly negative $\varepsilon_{Nd}(t)$ values (Fig. 6a) (e.g., Wang et al., 2006b, 2008b). In contrast, the Somka granodiorites have high positive $\varepsilon_{Nd}(t)$

values (Fig. 6a). In addition, adakitic rocks were formed by delaminated or subducting continental lower crust that generally occur in within-plate extensional or syn-collisional settings, respectively (e.g., Wang et al., 2006b, 2008b). However, the Somka granodiorites were generated in a Late Cretaceous arc setting (Jiang et al., 2012; Ma et al., 2013a, b, c).

The Somka granodiorites are also difficult to explain by melting of thickened lower crust (Mechanism D) because the resulting rocks generally have low MgO or $Mg^{\#}$ values (Fig. 3e and f) similar to those of experimental melts from metabasalts and eclogites (mostly $Mg^{\#} < 45$) (Rapp et al., 1999; Sen and Dunn, 1994). More specifically, previous studies have shown that adakitic rocks generated by melting of thickened lower crust beneath the GBST exhibit low $Mg^{\#}$ values (36–43) (Guan et al., 2012; Wen et al., 2008a), The Somka adakitic granodiorites and magnesian diorites, however, have higher and more variable $Mg^{\#}$ values (44–58) than those of metabasaltic and eclogite experimental melts.

Magmatic rocks generated by fractional crystallization processes generally exhibit continuous compositional trends from basaltic rocks derived from the mantle to felsic rocks derived from residual magmas (Castillo et al., 1999; Macpherson et al., 2006). However, the Somka adakitic granodiorites have different compositional trends compared to adakitic magnesian diorites in the Somka area and other coeval slab-derived adakites or adakitic magnesian diorites in southern Tibet (Figs. 3 and 4a) (Jiang et al., 2012; Ma et al., 2013c; Zhang et al., 2010a). Moreover, their compositional trend is inconsistent with the fractional crystallization trend of plagioclase, garnet and amphibole (Figs. 3d and 4b and c). In addition, the fractionation of olivine or pyroxene is not consistent with the depletion trend of HREE (e.g., Yb) of the Somka adakitic granodiorites and magnesian diorites. These minerals are unable to incorporate HREE, which generally leads to concave-upward HREE on chondrite-normalized REE concentration patterns (Castillo et al., 1999).

Crustal assimilation or magma mixing mechanisms usually require a crust-derived felsic end-member component with low $\varepsilon_{Nd}(t)$ values and high initial $^{87}Sr/^{86}Sr$ ratios and a mantle-derived basaltic end-member component with high $\varepsilon_{Nd}(t)$ values and lower initial $^{87}Sr/^{86}Sr$ ratios (Castillo et al., 1999; Guo et al., 2007b; Streck et al., 2007). Here, the most mafic dioritic rock sample (09TB117-1) (SiO_2 = 50.94 wt.%, $(^{87}Sr/^{86}Sr)_i = 0.7040$, $\varepsilon_{Nd}(t) = +3.6$) and the most felsic granite sample (09TB124) (SiO_2 = 74.2 wt.%, $(^{87}Sr/^{86}Sr)_i = 0.7040$, $\varepsilon_{Nd}(t) = +3.7$) in the Somka area most closely correspond to mantle-

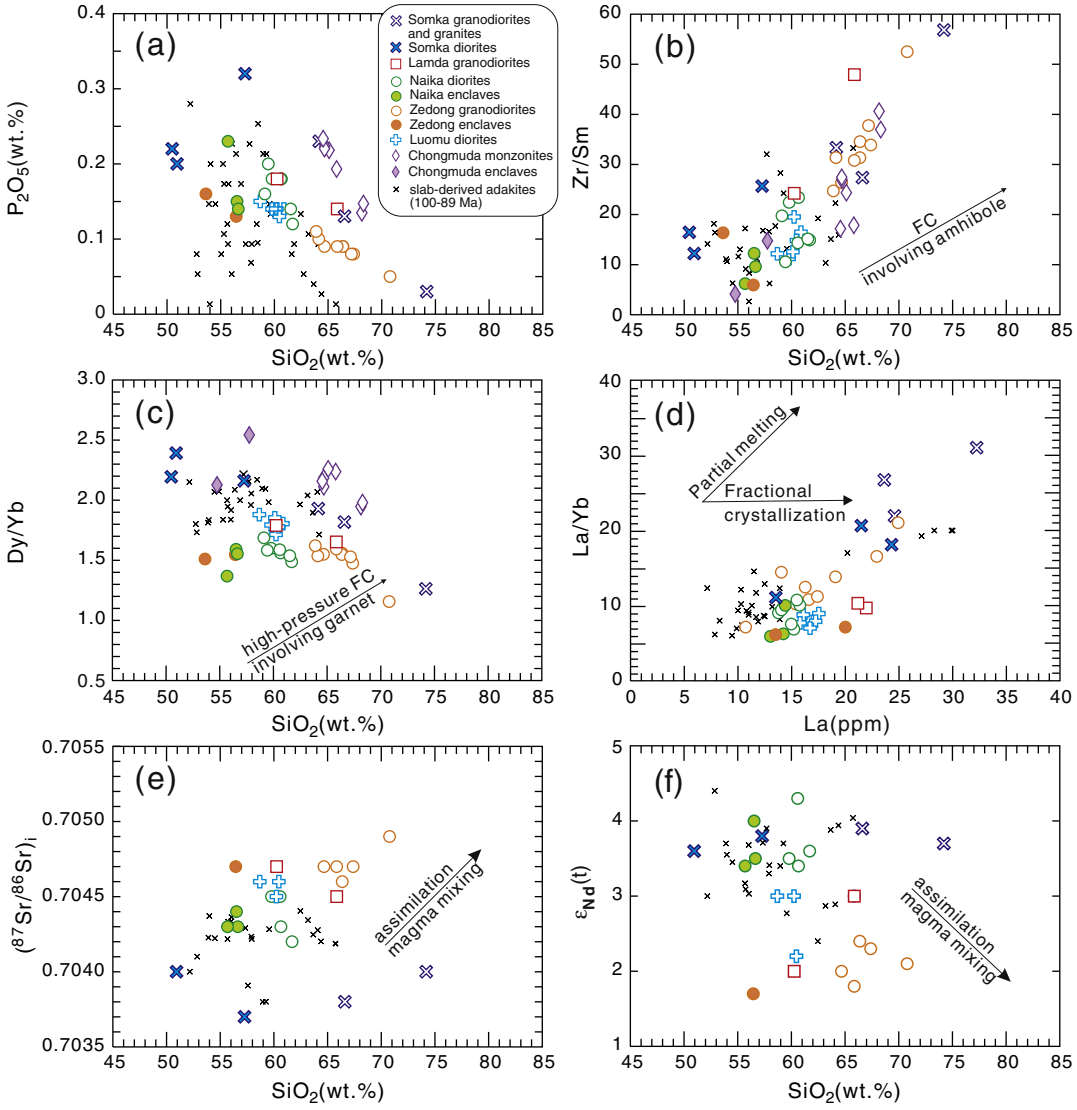

Fig. 4. (a) P_2O_5 versus SiO_2; (b) Zr/Sm versus SiO_2. Due to the incompatibility of Zr and compatibility of Sm in hornblende (Drummond et al., 1996), the fractional crystallization will cause an increase of Zr/Sm ratios in residual magmas; (c) Dy/Yb versus SiO_2; (d) La/Yb versus La; (e) $(^{87}Sr/^{86}Sr)_i$ versus SiO_2; and (f) $\varepsilon_{Nd}(t)$ versus SiO_2. The data for Cretaceous (100–89 Ma) slab-derived adakites in the southern Gangdese Belt are from Jiang et al. (2012), Ma et al. (2013c) and Zhang et al. (2010a).

derived and crust-derived magmas, respectively. However, the Somka adakitic granodiorites have slightly lower initial $^{87}Sr/^{86}Sr$ ratios (Fig. 4e and f), which is difficult to explain by crustal assimilation or magma mixing. In addition, the Somka granites and magnesian diorites have homogeneous zircon $\varepsilon_{Hf}(t)$ ($\Delta\varepsilon_{Hf}(t) < 5.0$) values (Fig. 7a and b), indicating that they could not be derived by magma mixing.

5.1.1.2. Partial melting of subducted oceanic crust (Mechanism A). We argue that the Somka adakitic granodiorites were most likely generated by partial melting of the subducted Neo-Tethyan Oceanic crust. First, studies on tectonics, sedimentation and magmatism in the Lhasa Block demonstrate that the Somka intrusive rocks were formed in an arc setting during the Late Cretaceous (Ji et al., 2009b; Jiang et al., 2012; Kapp et al., 2005, 2007; Ma et al., 2013a,b,c; Wen et al., 2008b). Second, the Somka adakitic granodiorites are geochemically similar to subducted oceanic crust-derived adakites. They exhibit trace element patterns similar to those of Cretaceous (~136–90 Ma) adakites derived from subducted Neo-Tethyan oceanic crust (Jiang et al., 2012; Ma et al., 2013c; Zhu et al., 2009) (Fig. 5a and b). They have relatively high $Mg^{\#}$ (44–51) values similar to those of slab-derived adakites in the GBST and elsewhere (Fig. 3e and f), indicating the interaction between slab-derived melts and mantle wedge peridotites during ascent. They have $\varepsilon_{Nd}(t)$ and $\varepsilon_{Hf}(t)$ values similar to those of Cretaceous slab-derived adakitic rocks in the GBST (Figs. 6a and 9a) (Jiang et al., 2012; Ma et al., 2013c; Zhu et al., 2009). Moreover, they also have $\varepsilon_{Nd}(t)$ values similar to those of Tethyan basalts (Fig. 6a) (Mahoney et al., 1998; Xu and Castillo, 2004; Zhang et al., 2005), and $\varepsilon_{Hf}(t)$ similar to those of Indian Ocean MORB (Fig. 6b) (Ingle et al., 2003).

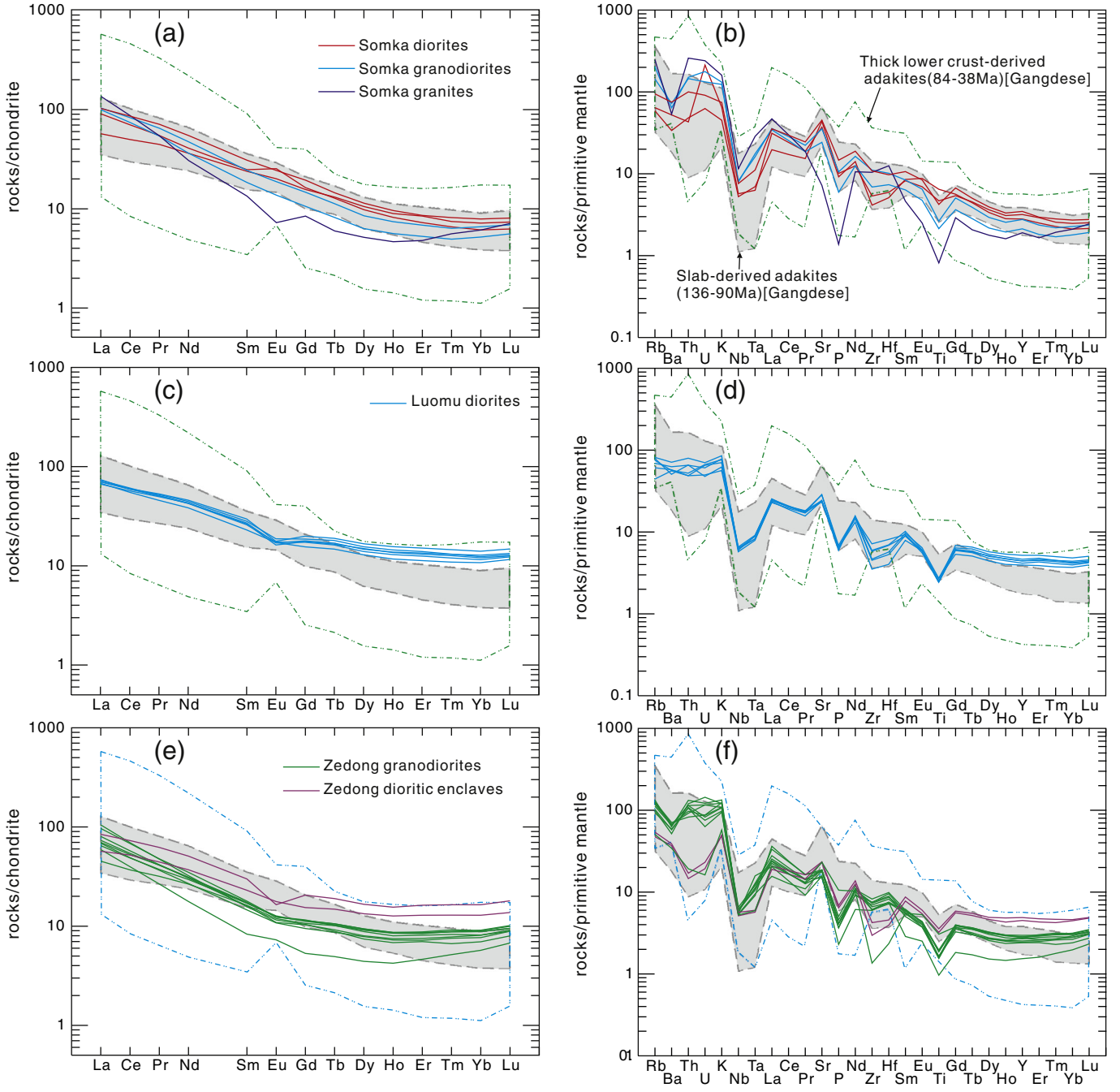

Fig. 5. Chondrite-normalized rare earth element (REE) patterns and primitive mantle-normalized rare earth element (REE) patterns for the Chanang–Zedong magmatic rocks. Chondrite and primitive mantle data are from Sun and McDonough (1989). The data are from the same source as in Fig. 3.

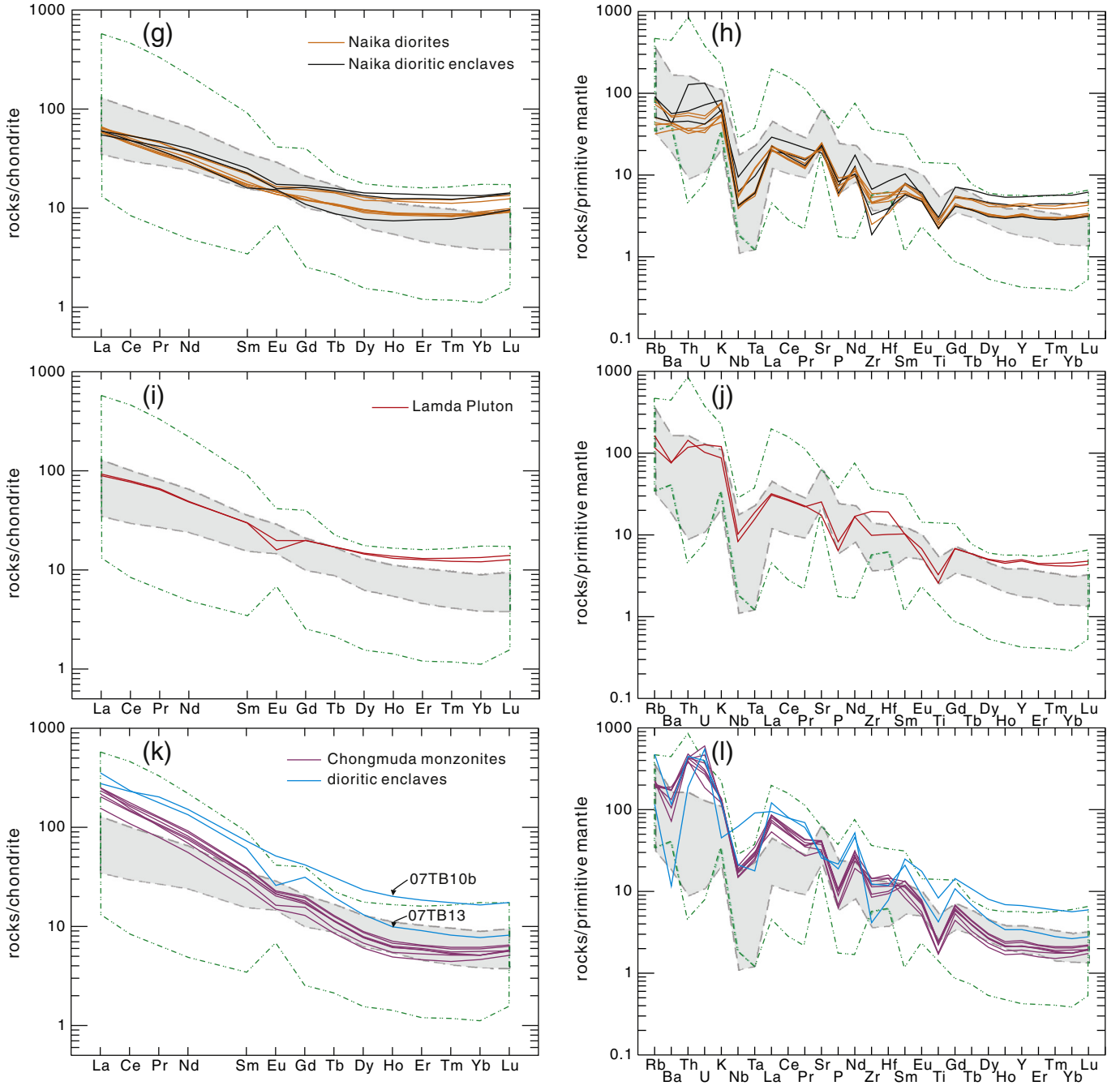

Fig. 5 (*continued*).

It is well documented that the composition of adakitic magmas in subduction zones are mainly controlled by contributions from the subducted oceanic crust, the overlying subducted sediments, and the mantle wedge (Castillo, 2012, and references therein). The Somka adakitic diorites have high Th/La ratios and Th contents and exhibit Nd–Hf isotope decoupling (Fig. 6b), suggesting that the source of the Somka granodiorites contained sedimentary components in addition to basaltic oceanic crust components (e.g., Jiang et al., 2012). Based on Sr–Nd isotopic composition model calculations, the Somka adakitic granodiorites may have been generated by partial melting of ~90% basaltic oceanic crust and ~10% oceanic sediments (Fig. 6a). Therefore, all lines of evidence suggest that they were most probably produced by partial melting of Neo-Tethyan basaltic oceanic crust and minor sediments, and subsequently underwent minor interaction with mantle wedge peridotite.

The Somka diorites have lower SiO_2 and higher MgO contents and $Mg^{\#}$ than those of the Somka adakitic granodiorites (Appendix 8) and are similar to adakitic magnesian andesites, which are generally considered to have been derived by the interaction between subducted oceanic crust-derived adakitic melts and mantle wedge peridotites (Escuder et al., 2007; Wang et al., 2008a).

5.1.1.3. Co-magmatic petrogenetic link between granodiorites and granites. In the field, the Somka granites, granodiorites and diorites exhibit gradual or transitional relationships, indicating that they formed coevally. Zircon U–Pb dating confirms that they formed contemporaneously in

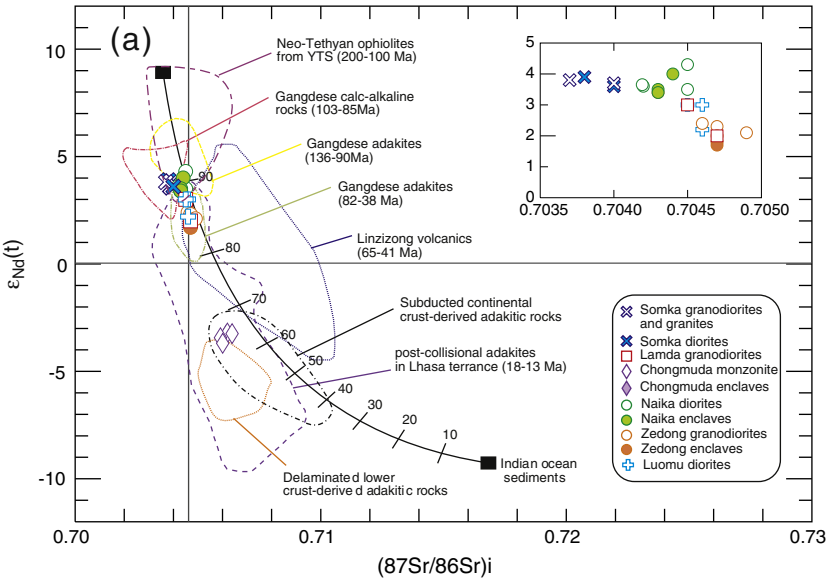
(a)
Neo-Tethyan ophiolites from YTS (200-100 Ma)
Gangdese calc-alkaline rocks (103-85Ma)
Gangdese adakites (136-90Ma)
Gangdese adakites (82-38 Ma)
Linzizong volcanics (65-41 Ma)
Subducted continental crust-derived adakitic rocks
post-collisional adakites in Lhasa terrance (18-13 Ma)
Delaminated lower crust-derived adakitic rocks
Indian ocean sediments
Somka granodiorites and granites
Somka diorites
Lamda granodiorites
Chongmuda monzonite
Chongmuda enclaves
Naika diorites
Naika enclaves
Zedong granodiorites
Zedong enclaves
Luomu diorites
εNd(t)
(87Sr/86Sr)i

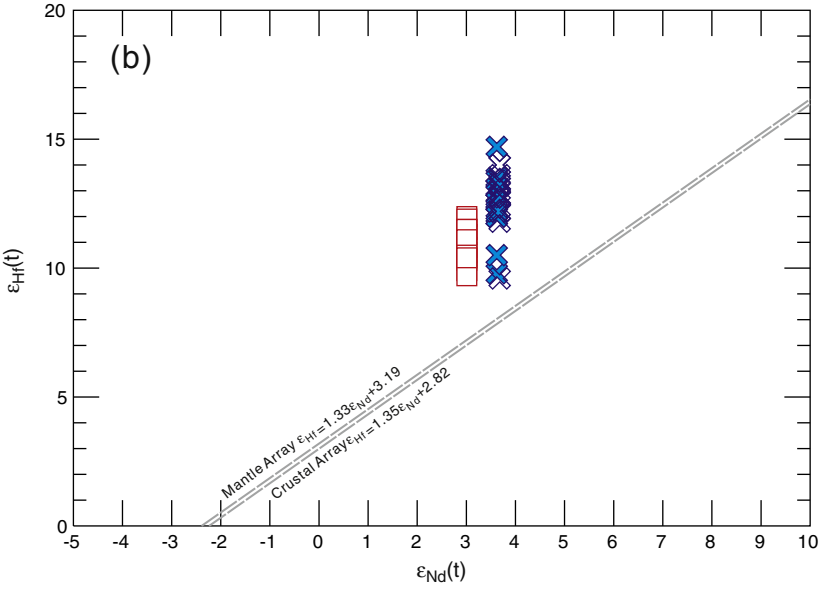
(b)
Mantle Array εHf=1.33εNd+3.19
Crustal Array εHf=1.35εNd+2.82
εHf(t)
εNd(t)

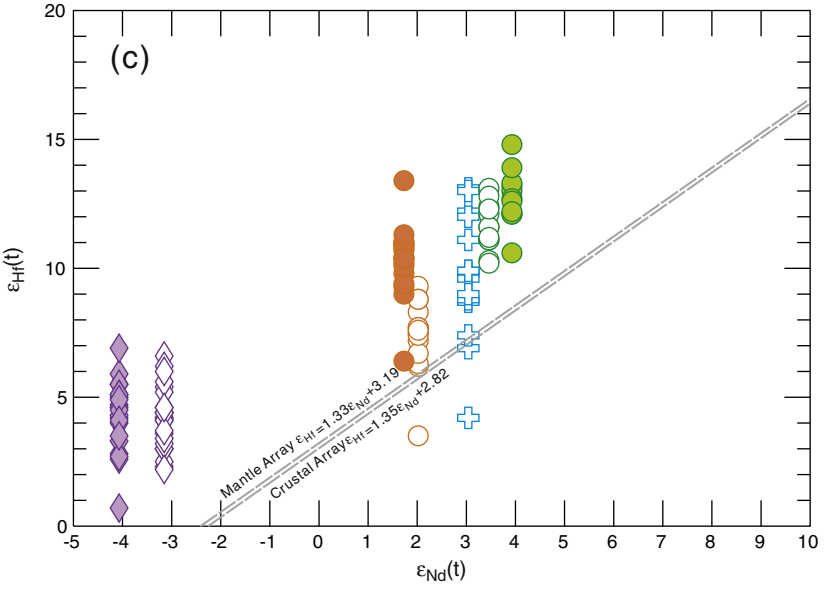
(c)
Mantle Array εHf=1.33εNd+3.19
Crustal Array εHf=1.35εNd+2.82
εHf(t)
εNd(t)

the Late Cretaceous (~91 Ma). Geochemically, the granite sample (09TB124) has distinctly higher SiO_2 and lower MgO and Sr contents than the granodiorites and displays significant negative P, Ti and Eu anomalies (Fig. 5a and b). These features indicate that the granite may have been produced by fractional crystallization (plagioclase + hornblende + apatite) (Castillo et al., 1999). The granite has lower Sc, Ti, V, Cr and Ni concentrations and higher Zr/Sm ratios than the Somka granodiorites. Due to the incompatibility of Zr and compatibility of Sm, V, Sc, Cr and Ni in hornblende (Ewart and Griffin, 1994; Sisson, 1994), its fractional crystallization will cause an increase in Zr/Sm ratios and a decrease in Sc, V, Cr and Ni in residual granitic magmas. In addition, the obvious MREE depletion in the granite (Fig. 5a) also indicates fractional crystallization of hornblende (Castillo et al., 1999). Thus, differentiation from granodioritic to granitic magmas was probably controlled by fractional crystallization.

5.1.2. ~62 Ma

5.1.2.1. Mechanisms A–C and E–F. In general, adakitic rocks generated by mechanisms A–C have high $Mg^{\#}$ values (>47–50) or are similar to high-Mg andesites in that their MgO or $Mg^{\#}$ values were increased by the interaction of magmas derived from subducted oceanic, subducted continental crust or delaminated lower crust with mantle peridotites during magma ascent (Fig. 3e and f) (Rapp et al., 1999; Wang et al., 2006a,b, 2008a,b). However, the Naika and Zedong adakitic rocks have low $Mg^{\#}$ (36–46) values (Fig. 3e and f), indicating that such interaction was unlikely. In addition, they exhibit positive $\varepsilon_{Nd}(t)$ values (Fig. 6a) that are also inconsistent with those ($\varepsilon_{Nd}(t) < 0$) of adakitic rocks derived from delamination or subducting continental lower crust (e.g., Wang et al., 2006b, 2008b).

The Naika and Zedong adakitic rocks could also not have been generated by high- or low-pressure factional crystallization from parental basaltic magmas (Mechanisms E). Given that high-pressure fractional crystallization involving garnet will cause a decrease in HREE and Y contents while the Sr/Y and Dy/Yb ratios in the residual magmas increase with increasing SiO_2 contents (Macpherson et al., 2006). However, these samples do not show such trends in their chondrite-normalized rare earth element patterns (Fig. 5e and g) or on a Dy/Yb vs. SiO_2 diagram (Fig. 4c). During low-pressure fractional crystallization involving olivine and pyroxene, the derived magmas should show a clear decrease in Cr, Ni contents and $Mg^{\#}$ values with increasing SiO_2 (Castillo et al., 1999), but their $Mg^{\#}$ values are relatively constant and inconsistent with either fractional crystallization or AFC processes (Fig. 3f). Moreover, both the Naika and Zedong adakitic rocks and their respective associated enclaves have similar Sr–Nd isotopic compositions, which is inconsistent with a crustal assimilation model (Castillo et al., 1999). In addition, a plot of La/Yb vs. La shows that partial melting rather than fractional crystallization played a key role in their formation (Fig. 4d). It is also unlikely that they were generated by magma mixing between felsic and basaltic magmas (Mechanism F). The adakitic host rocks and mafic enclaves have similar Sr–Nd–Hf isotopic compositions (Figs. 6a and 7d and h), inconsistent with the magma mixing model (Yang et al., 2007).

5.1.2.2. Partial melting of juvenile thickened lower crust (Mechanism D). The Naika and Zedong adakitic rocks were most probably generated by partial melting of a thickened lower crust, based on the following evidence. First, they have MgO contents and $Mg^{\#}$ values, similar to those of experimental melts of metabasaltic rocks in equilibrium with eclogitic melts at high pressures of 1.0–4.0 GPa (Fig. 3e and f) or adakitic rocks derived from thickened lower crust (Chung et al., 2003, 2009). Second, their arc-like element patterns (Fig. 5e and g) and positive $\varepsilon_{Nd}(t)$ (Fig. 6a) values with relatively young Nd model ages (0.49 to 0.70 Ga) suggest that they originated from younger arc-type crustal rocks (Ji et al., 2009b; Wen et al., 2008a). The Gangdese Belt is a part of the southern Lhasa Block, which is dominated by juvenile crust resulting from underplating of mantle-derived mafic magmas (Ji et al., 2009a,b; Ma et al., 2013b). The Sr–Nd isotopic compositions of the Naika and Zedong rocks are very similar to the Late Cretaceous (~83–80 Ma) thickened lower crust adakites (Wen et al., 2008a) and Cretaceous granitoids (Ji et al., 2009a) in the GBST (Fig. 6a). In addition, the $\varepsilon_{Hf}(t)$ values of their ~62 Ma zircons are also consistent with those of Cretaceous granitoids in the GBST (Ji et al., 2009a,b) (Fig. 9a). These observations suggest that they were most likely derived by partial melting of juvenile thickened lower crust.

Experimental studies have suggested that melting of mafic materials produces adakitic magma at high-pressure or deep crustal levels (>1.2 GPa, corresponding to >40 km), with a residual phase containing garnet but no plagioclase (Rapp and Watson, 1995; Rapp et al., 1999). The presence of residual garnet in the source will result in a strong HREE depletion in resultant magmas. If amphibole is also a residual phase, then it will induce concave-upward patterns between middle and heavy REE because of its high partition coefficients for these elements in intermediate to felsic melt (Huang et al., 2009). The lack of strongly HREE-depleted patterns for the Naika and Zedong adakitic rocks (Fig. 5e and g) is thus indicative of dominant amphibole with minor garnet in the residue (Gromet and Silver, 1987), indicating that garnet amphibolite rather than eclogite is a more likely source rock. Their zircon $\varepsilon_{Hf}(t)$ values deviate from the whole-rock $\varepsilon_{Nd}(t)$ values of the average mantle and crust Hf–Nd isotope evolution arrays (Vervoort et al., 1999) (Fig. 6c), suggesting some Hf–Nd isotope decoupling. The deviation between Hf and Nd isotopes in granites is generally attributed to high Lu/Hf ratios in magmas formed by melting in the presence of garnet or by garnet fractional crystallization during magma emplacement (Vervoort et al., 2000; Zhao et al., 2008). Alternatively, such Hf–Nd isotopic deviation could also be due to refractory zircons that preserve their initial Hf isotope compositions (Wu et al., 2006).

As noted above, the Naika and Zedong adakitic rocks are mainly derived from partial melting of juvenile thickened lower crust. However, a detailed comparison between them reveals some differences (Figs. 3, 6 and 7). The major geochemical differences are summarized in Appendix 11.

(1) The Zedong adakitic granodiorites (ZDAG) have high K_2O and their K_2O/Na_2O ratios vary from 0.87 to 1.32 (with most >1) (Fig. 8). The high K_2O/Na_2O ratios, coupled with relatively low Al_2O_3 contents (14.8–16.2 wt.%), are generally consistent with adakitic rocks generated by old and water-absent or sediment-bearing thickened lower crust (Wang et al., 2008b). In contrast, the Naika adakitic diorites have distinctly lower K_2O and K_2O/Na_2O ratios varying from 0.38 to 0.73, similar to those of GBST adakites derived from thickened water-bearing juvenile lower crust (Wen et al., 2008a). Fractional crystallization of amphibole (Rapp and Watson, 1995; Sen and Dunn, 1994) can cause a decrease of K concentration in the melt and produce low-K silicic melts. On a Zr/Sm vs. SiO_2 diagram (Fig. 4b), the Zedong and Naika adakitic rock samples show obvious linear trends, indicating that fractional crystallization of amphibole might have taken place, which would imply that the

Fig. 6. (a) $\varepsilon_{Nd}(t)$ vs. $(^{87}Sr/^{86}Sr)_i$ diagram for the Chanang–Zedong intrusive rocks. Data sources: Yarlung Tsangpo ophiolites (Guilmette et al., 2009; Miller et al., 2003; Xu and Castillo, 2004; Zhang et al., 2005), Gangdese calc-alkaline rocks (Wen et al., 2008a), Linzizong volcanic rocks (Mo et al., 2007, 2008), post-collisional adakites in the Lhasa Block (18–13 Ma) (Guo et al., 2007a; Hou et al., 2004), subducted continental crust-derived adakitic rocks in the Qiangtang Block (Wang et al., 2008b), and delaminated lower crust-derived adakitic rocks in the eastern Yangtze Block (Wang et al., 2006a,b). The data for the Gangdese adakites are the same source as in Fig. 3. (b) and (c) Zircon $\varepsilon_{Hf}(t)$ vs. whole-rock $\varepsilon_{Nd}(t)$ diagram. Field of Hf–Nd data for Indian MORB is from Ingle et al. (2003). The mantle and crustal array are from Vervoort et al. (1999).

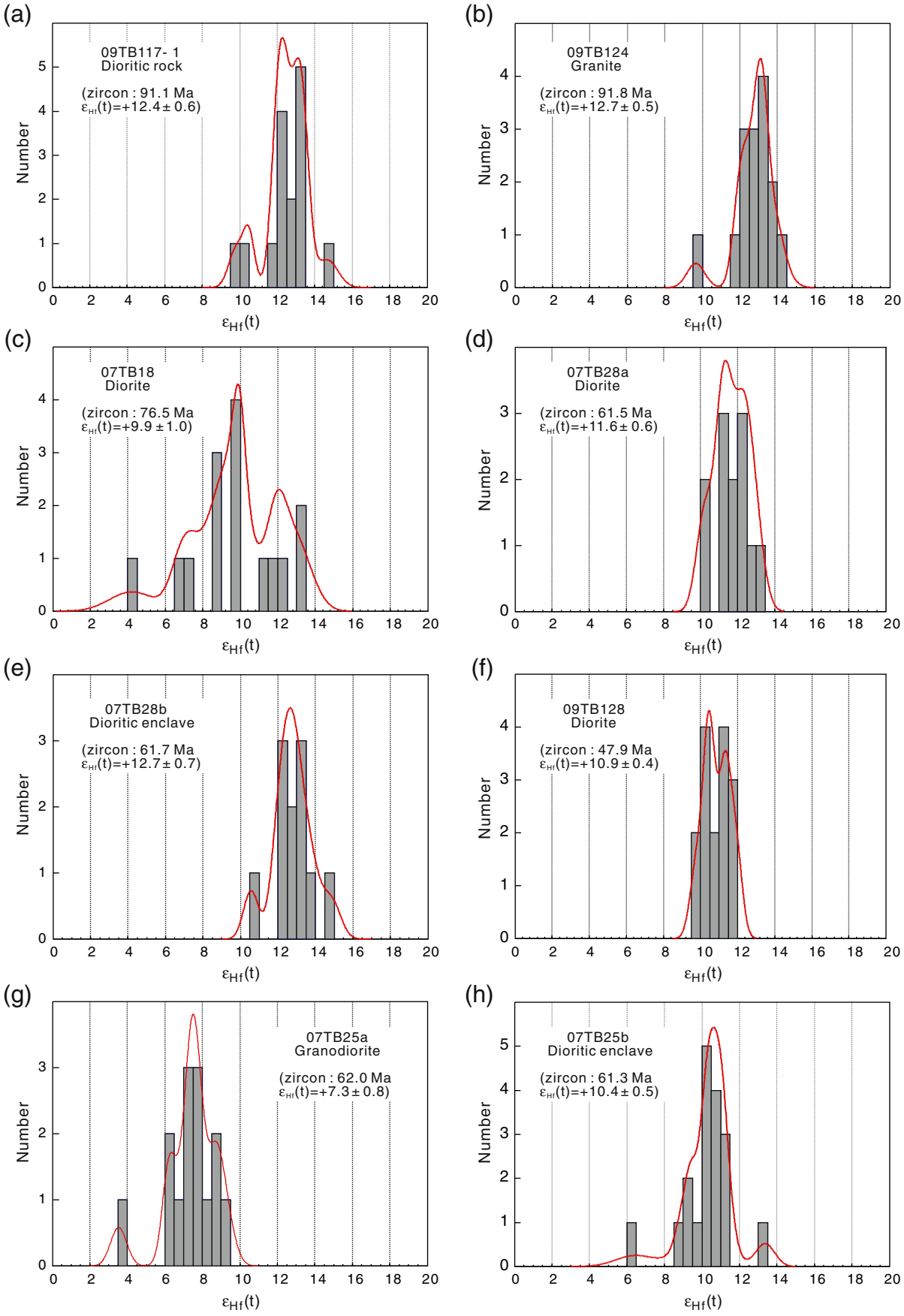

Fig. 7. Histogram of initial Hf isotope ratios for the intrusive rocks in the Chanang–Zedong area, southern Tibet.

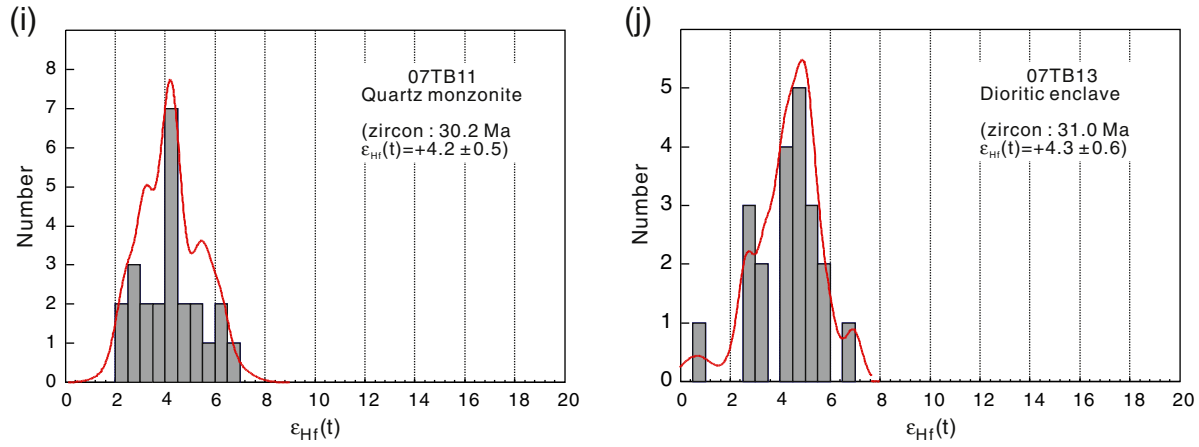

Fig. 7 (*continued*).

resulting residual melts should have relatively low K_2O contents and K_2O/Na_2O ratios. The Zedong adakitic rocks, however, have higher SiO_2 and higher K_2O and K_2O/Na_2O ratios compared to the coeval Naika adakitic rocks. Thus, the compositional differences between the two suites most plausibly resulted from differences in their sources, rather than amphibole fractional crystallization in a common parental magma.

(2) The Zedong adakitic rocks have lower $\varepsilon_{Nd}(t)$ and $\varepsilon_{Hf}(t)$ values than the Naika adakitic rocks (Figs. 6a and c and 8b and c). Jurassic–Cretaceous granitoids of the Gangdese area commonly have high and positive $\varepsilon_{Nd}(t)$ (mostly >3.0) and $\varepsilon_{Hf}(t)$ (mostly >10.0) (Ji et al., 2009a,b; Zhu et al., 2011), indicating that the Gangdese Belt mainly consists of juvenile crust. Aitchison et al. (2000) and McDermid et al. (2002) proposed that rocks of the Zedong area correspond to a Late Jurassic–Early Cretaceous intra-oceanic island arc setting. Based on the studies of Late Jurassic (~160 Ma) adakitic rocks with high $\varepsilon_{Nd}(t)$ in the Zedong area (Fig. 8b and c), Wei et al. (2007) inferred the existence of a Zedong intra-oceanic island arc within Tethys. Recent petrological and geochemical data from the Zhongba ophiolite reveal the presence of a large intra-oceanic subduction system within Neo-Tethys during the Early Cretaceous between the Indian and Lhasa blocks (Dai et al., 2011). Therefore, the Zedong area should contain juvenile Jurassic–Cretaceous intraoceanic arc crust. The relatively low $\varepsilon_{Nd}(t)$ and $\varepsilon_{Hf}(t)$ values of the ~62 Ma Zedong adakitic rocks (Fig. 8b), however, suggest that their source included enriched crustal components. We propose that these components were most likely derived from old Indian continental crust material. As the Zedong pluton occurs closer to the Yarlung–Tsangpo suture zones than the Naika pluton (Fig. 1b), we suggest that the former was probably derived by partial melting of the mixture of juvenile southern Lhasa continental crust and old Indian continental crust.

5.1.2.3. Co-magmatic petrogenetic link between the host rocks and enclaves. Although the dioritic enclaves and their host rocks have consistent whole-rock initial $^{87}Sr/^{88}Sr$ and $\varepsilon_{Nd}(t)$ values (Fig. 6a and c), their zircon $\varepsilon_{Hf}(t)$ values are distinct, indicating that they may have been derived from different sources. Mafic microgranular enclaves (MMEs of Didier and Barbarin, 1991) are common in most granitoids, and genetic models applied to them include origins as: (1) residues after partial melting of crust, which is the source of granitic magma (Chappell et al., 1987), (2) xenoliths of the country rocks or accumulations formed by early crystallization of mantle-derived magma that evolved into granitic magma by fractional crystallization (FC) (Shellnutt et al., 2010), and (3) the products of mixing between felsic and mafic magma derived from crustal and mantle sources, the mafic enclaves thus representing inclusions of mafic magma, albeit extensively modified (Yang et al., 2007 and references therein). Generally, country rock xenoliths should have different zircon U–Pb ages from their host rocks. However, our zircon U–Pb dating for the mafic enclaves and Naika and Zedong host plutons show that they have coeval emplacement ages (Fig. 2d and e and g and h). The mafic enclaves and granitoids, however, also have different Hf isotopic compositions, precluding the fractional crystallization and restite model. In addition, garnet is absent in these enclaves but is a common residual mineral in the sources of adakitic magma (Defant and Drummond, 1990). Here, we suggest that the mafic enclaves from the Naika and Zedong pluton reflect hybridization between mantle-derived mafic and crust-derived felsic magmas. The igneous texture of the mafic enclaves, including needle-like apatite in the matrix, growth of plagioclase phenocrysts with oscillatory-zoning, and local K-feldspar megacrysts, indicate that the mafic microgranular enclaves represent external magmatic globules that were injected into the felsic host magmas before they solidified (e.g., Yang et al., 2007).

5.1.3. ~30 Ma

Harrison et al. (2000) first reported ~ 30 Ma magmatism in the Yajia area, which is adjacent to the Chongmuda pluton (Fig. 1d). Detailed studies of the Yajia and Chongmuda intrusive rocks have demonstrated that they both have geochemical affinities with adakitic rocks and negative $\varepsilon_{Nd}(t)$ and low zircon $\varepsilon_{Hf}(t)$ values (Chung et al., 2009; Hou et al., 2012; Jiang et al., 2011; Zheng et al., 2012). It has been proposed that these Oligocene (~30 Ma) rocks were derived by partial melting of juvenile thickened lower crust beneath the Gangdese arc (Chung et al., 2009; Zheng et al., 2012). However, our earlier work suggested that they were more plausibly derived from partial melting of subducted Indian continental lower crust (Mechanism C) (Jiang et al., 2011), rather than from the juvenile lower crust under the GBST. Recently, Hou et al. (2012) also proposed that the source of these adakitic rocks is thickened Indian mafic lower crust. We suggest that Mechanism C for ~30 Ma adakitic rocks is supported by the following lines of evidence.

(1) Geophysical data reveal that the Indian lithosphere was underthrust beneath the Lhasa Block as far north as the Bangong–Nujiang suture, following the India–Eurasian continental collision in the early Paleocene. Thus, tectonic events make feasible the possibility that the Chongmuda adakitic rocks could have been derived by partial melting of the northward subducted Indian mafic lower crust during the Oligocene (Nabelek et al., 2009; Schulte-Pelkum et al., 2005; Tapponnier et al., 2001).

(2) Late Jurassic to early Eocene granitoids of the Gangdese Belt are commonly characterized by positive $\varepsilon_{Nd}(t)$ (> +3.0), which indicates that the Gangdese lower crust was dominated by juvenile

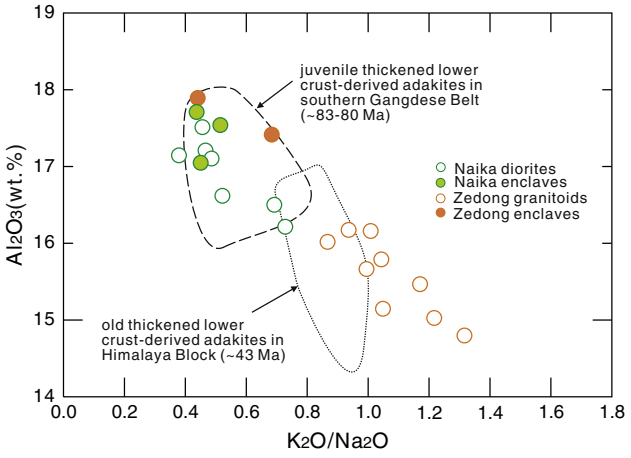

Fig. 8. Al_2O_3 vs. K_2O/Na_2O. The fields for juvenile thickened lower crust-derived adakites in southern Gangdese Belt and old thickened lower crust-derived adakites in the Himalayan Block are constructed in terms of data from Wen et al. (2008a) and Zeng et al. (2011).

crustal materials derived by underplating of mafic mantle-derived magmas (Ji et al., 2009b; Ma et al., 2013b). In contrast, the Oligocene (~30 Ma) Chongmuda adakitic rocks emplaced in the southern Gangdese Belt have significantly more negative $\varepsilon_{Nd}(t)$ (Fig. 6a) and low $\varepsilon_{Hf}(t)$ (Figs. 6c and 7i and j). The most reasonable interpretation of such an enriched component is that the Chongmuda rocks were derived from northward subducted old Indian continental lower crust with negative $\varepsilon_{Nd}(t)$ and low $\varepsilon_{Hf}(t)$ values (Jiang et al., 2011). Compared, however, to the Eocene thickened-crust adakitic rocks in the Northern Himalayan Block ($\varepsilon_{Nd}(t)$ values of −8.9 to −15.0) (Hou et al., 2012; Zeng et al., 2011), the Chongmuda adakitic rocks have relative high $\varepsilon_{Nd}(t)$ values. Collectively, the evidence suggests that the Indian lower crust-derived Chongmuda magmas were contaminated by the overlying depleted mantle beneath the southern Lhasa Block during ascent (Jiang et al., 2011).

(3) Geochemical characteristics of the Chongmuda mafic enclaves also support the northward subduction of Indian continental crust. The enclaves include both high silica–high magnesian and low silica–Nb rich rocks. This combination of adakitic rocks, magnesian andesites (or diorites) and Nb-enriched basaltic rocks is a common arc rock assemblage (Escuder et al., 2007; Wang et al., 2008a). The adakites, magnesian andesites and Nb-enriched basaltic rocks have, respectively, been interpreted as subducted slab-derived magmas, hybridization magmas of adakitic melts with mantle peridotite, and magmas originating from slab melt-metasomatized mantle wedge peridotites (Castillo, 2012; Defant and Drummond, 1990; Escuder et al., 2007). The high silica–high magnesian enclaves in the Chongmuda adakitic rocks have geochemical affinities with magnesian andesites and were probably generated by the interaction of subducted old Indian continental crust-derived adakitic melt and mantle peridotites. The low silica–Nb rich enclaves in the Chongmuda adakitic rocks are similar to Nb-enriched basaltic rocks, and therefore may have been produced from mantle peridotites metasomatized by subducted Indian continental crust-derived adakitic melts (Jiang et al., 2011).

5.2. Other intrusive rocks

5.2.1. ~77 Ma and ~48 Ma

The Luomu (~77 Ma) and Lamda (~48 Ma) intrusive rocks are not adakitic in composition, but they have similar major and trace element (Figs. 3 and 5) and Sr–Nd isotopic compositions (Fig. 6a), indicating that they were derived from comparable sources. We propose that both the Luomu and the Lamda magmas were probably generated by partial melting of juvenile arc crust beneath the GBST.

(1) The Luomu and Lamda intrusive rocks have moderate SiO_2 and low MgO, $Mg^{\#}$, Cr and Ni contents, similar to GBST Jurassic–Early Eocene calc-alkaline granitoids considered to have been derived from juvenile continental crust (Ji et al., 2009a). Trace element and REE patterns of the Luomu and Lamda intrusive rocks are also similar to those of classic arc-type granitoids, i.e., enriched large ion lithophile elements (LILEs: Rb, Ba, Th, U, K) and light rare earth elements (LREEs: La, Ce) and relatively depleted high field strength elements (HFSEs: Nb, Ta, Ti). The depletion of Eu can be explained either by the fractional crystallization of plagioclase or the retention of residual of plagioclase in the source, while the depletion of P might reflect the crystallization of apatite. The Luomu and Lamda intrusive rocks exhibit relatively flat HREE patterns in most samples (Fig. 5c and i), suggesting that amphibole played an important role during partial melting as a residual phase in the source.

(2) Both the Luomu and Lamda intrusive rocks have $(^{87}Sr/^{86}Sr)_i$ and $\varepsilon_{Nd}(t)$ values with young Nd model ages (620–770 Ma), consistent with those of the Jurassic–Cretaceous calc-alkaline granitoids in the GBST. In particular, they have $(^{87}Sr/^{86}Sr)_i$, $\varepsilon_{Nd}(t)$ and Nd model age (510–750 Ma) values similar to those of Late Cretaceous (83–80 Ma) adakitic granodiorites originating from partial melting of newly underplated mafic lower crust (Wen et al., 2008a). This suggests that the Luomu and Lamda plutons also originated from the melting of juvenile arc-type crustal rocks (Chu et al., 2011; Wen et al., 2008a; Zhu et al., 2011 and references therein).

6. Geodynamic processes

6.1. ~100–65 Ma slab roll-back

Previous studies indicated that an early Late Cretaceous (ca. 100–80 Ma) magmatic "flare-up" occurred in the southern Lhasa Block (Ji et al., 2009b; Ma et al., 2013a,b,c; Wen et al., 2008b). The proposed triggering mechanisms for these magmatic events include normal-angle subduction (100–85 Ma) and subsequent low-angle or flat oceanic slab subduction (85–80 Ma) (Wen et al., 2008a, b), oceanic ridge subduction (Zhang et al., 2010a) and roll-back of subducted oceanic slab (Ma et al., 2013a,c).

The most recent studies suggest that early Late Cretaceous slab roll-back following low-angle or flat-slab subduction in the Early Cretaceous can best account for the contemporary Gangdese magmatic "flare-up" and subsequent underplating of mafic magmas (Ma et al., 2013a,c). First, extensive zircon U–Pb dating shows that most of the Late Jurassic–Early Cretaceous magmatic rocks occur in the central and north Lhasa Block (Zhu et al., 2013 and references therein) while Late Cretaceous magmatic rocks occur widely in the southern Lhasa Block (Zhu et al., 2013). The development of magmatism in the Lhasa Block suggests that the magmatic front moved farther north due to flat or low-angle subduction in the Early Cretaceous (Kapp et al., 2005; Zhang et al., 2012). Second, high-temperature (up to 1340 °C) norites in the Milin area were derived from asthenosphere–lithosphere interaction that was most plausibly due to asthenospheric upwelling resulting from the roll-back of subducted Neo-Tethyan oceanic slab (Ma et al., 2013a). The upwelling would also have provided enough heat for the partial melting of subducted oceanic slab, which generated adakitic rocks in the Somka and Milin areas (Ma et al., 2013c). For example, the calculated zircon-derived magma temperatures (T_{Zr} = 708–764 °C) for the Somka adakitic rocks are consistent with the requirements for slab melting (Sen and Dunn, 1994). The coeval occurrence of granulite-facies metamorphism (Zhang et al., 2010b) in the Milin area provides additional strong evidence for an early Late Cretaceous regional thermal

event, consistent with asthenospheric upwelling as a result of slab rollback (Ma et al., 2013a,c).

Late Cretaceous (90–77 Ma) magmatic rocks (Ji et al., 2009b; Wen et al., 2008b; Zhang et al., 2012; this study) occur in the GBST and were mainly derived by remelting of juvenile Gangdese arc crust during Neo-Tethyan oceanic crust subduction (Ji et al., 2009a,b; Wen et al., 2008a,b). Based on zircon U–Pb age data, Wen et al. (2008b) suggested that Gangdese magmatism was active in the Late Cretaceous (ca. 103–80 Ma) and Early Paleogene (ca. 68–43 Ma), but with a magmatic gap or quiescent period between ca. 80 and 68 Ma. However, detrital zircon U–Pb age data from the Xigaze fore-arc basin suggests that this magmatic gap did not exist and that continuous magmatism actually did occur during the Late Cretaceous (Wu et al., 2010). Our identification of the ~77 Ma Luomu diorites further supports the continuous nature of magmatism in the region.

The Cretaceous–Early Tertiary Gangdese arc in southern Tibet is generally attributed to the northward subduction of Neo-Tethyan oceanic lithosphere prior to India–Asian collision (Ji et al., 2009b; Kapp et al., 2007; Wen et al., 2008b). Some authors have also proposed that Cretaceous–Tertiary crustal shorting, basin development and volcanism in the Lhasa Block were mainly associated with the northward subduction of the Neo-Tethyan oceanic lithosphere (Kapp et al., 2005, 2007). During the Late Cretaceous to Eocene, the convergence rate between the Indian and Asian plates exceeded 10 cm/year (e.g., Lee and Lawver, 1995) and coincided with the onset of prolonged rollback (Fig. 10a) and steepening of the Neo-Tethyan oceanic slab during the Late Cretaceous (Lee et al., 2009, 2012; Ma et al., 2013c).

6.2. 65–60 Ma initial collision between Indian and Asian continents

The Yarlung–Tsangpo suture zone formed when the Indian continental landmass collided with the southern flank of Eurasia during the early Cenozoic (Yin and Harrison, 2000). However, the timing of initial collision remains a topic of debate (70–34 Ma) (Aitchison et al., 2007; Najman et al., 2010; Yi et al., 2011; Yin and Harrison, 2000). Many workers believe that the initial collision took place at ~65–60 Ma, based on studies of paleomagnetic data, sedimentation and magmatism in southern Tibet (Cai et al., 2011; Chu et al., 2011; Ding et al., 2005; Hu et al., 2012; Mo et al., 2007; Yi et al., 2011). For instance, based on the study of latest Paleocene sedimentary rocks from the Tethyan Himalaya on the northern margin of the Indian Plate and Lhasa Block, Patzelt et al. (1996) suggested that initial contact of the northern Indian margin with the Lhasa Block occurred at 65–60 Ma. A similar conclusion was reached by Yi et al. (2011), who proposed that the initial contact between the Tethyan Himalaya and Lhasa blocks took place before ca. 61 Ma based on paleomagnetic data from Early Paleogene marine sediments in southern Tibet. Based on evidence for uppermost Cretaceous to Eocene marine sedimentary sequences both to the south and north of the Yarlung–Tsangpo suture, and the record of ophiolite obduction, Ding et al. (2005) and Cai et al. (2011) tentatively supported initial collision between India and Asia at ~65 Ma rather than 65 Ma intra-oceanic arc subduction followed by later collision. In addition, based on combined stratigraphic, sedimentological, subsidence and provenance data for the Cretaceous–Paleogene succession from the Zhepure Mountain of southern Tibet, Hu et al. (2012) suggested that the collision of India with Asia occurred before the Late Danian (ca. 62 Ma). Mo et al. (2007) also suggested that the unconformity between the Linzizong volcanic sequence and the underlying Cretaceous rocks at ~65 Ma represents the initial India–Asia collision. Based on the studies of Paleogene granitoids exposed in the Gangdese batholith, Chu et al. (2011) also concluded that the continental collision of India with Asian should have started up to 5–6 m.y. earlier than 55 Ma.

Our study of the Early Paleogene (~62 Ma) adakitic rocks in the Zedong–Naika area leads to a new constraint on Tibetan tectonic evolution. As mentioned above, the Zedong and Naika plutons are located on the north side of the Yarlung–Tsangpo suture (Fig. 1c and d). Both were derived by partial melting of juvenile thickened lower crust. However, the Zedong adakitic rocks, located closer to the Yarlung–Tsangpo suture, have more enriched Nd–Hf isotopic compositions than the Naika adakitic rocks located slightly farther from the suture (Fig. 9), indicating that the source materials for the Zedong adakitic magmatism probably contained some old Indian continental crust components. Therefore, based on the combined evidence from the variable isotopic compositions of the Zedong and Naika adakitic magmas and previous studies, we suggest that the initial contact between the northern margin of the Indian Plate and the Lhasa Block most likely occurred at around ~65–62 Ma, rather than at ca. 50 Ma (e.g., Najman et al., 2010; Sun et al., 2012). This conclusion is also supported by previous studies on zircon Hf isotopes of Gangdese granitoids (Chu et al., 2011; Ji et al., 2009b). The zircon Hf isotopic compositions of Paleogene (ca. 55–50 Ma) Gangdese granitoids (Fig. 9a) exhibit obvious negative $\varepsilon_{Hf}(t)$ values, contrasting strongly with those of Jurassic/Cretaceous magmatic zircons. The marked decrease in $\varepsilon_{Hf}(t)$ values for the Paleogene zircons was interpreted as a result of source contamination by subducted Himalayan sediments, requiring that the India–Asia collision commenced before, and possibly up to 5–6 m.y. earlier than, 55 Ma (Chu et al., 2011; Ji et al., 2009b).

However, the heat source required for the partial melting of thickened lower crust required to generate the Early Paleogene Naika and Zedong adakitic rocks remains unresolved. The Linzizong volcanic successions show a geographical distribution, ages and geochemical features similar to the early Tertiary Gangdese granitoids, suggesting that both may have been products of the same transition from northward subduction of the Neo-Tethyan oceanic slab to collision between India and Asia (Mo et al., 2007). Lee et al. (2009, 2012) suggested that the early stages of Linzizong volcanism resulted from Neo-Tethyan slab rollback (Fig. 10b). Furthermore, the model of slab rollback is consistent with regional geologic data such as the Cretaceous–Tertiary shortening history of the central Lhasa Block (Kapp et al., 2005; Lee et al., 2009). Other potential mechanisms, however, such as the beginning of slab breakoff, could also provide the required heat source. If slab breakoff started at ca. 62 Ma, then melting of thickened lower crust beneath southern Tibet could have been triggered by the initial asthenospheric upwelling through the slab window. The time interval (~15–12 Ma) between initial continental collision (~65–62 Ma) or initial slab breakoff (~62 Ma) and completed breakoff (~50 Ma) (Lee et al., 2009, 2012) is consistent with numerical simulations that suggest oceanic slab breakoff generally occurs 10–20 Myr after continental collision (van Hunen and Allen, 2011).

6.3. 60–40 Ma slab break-off

We suggest that the ca. 50 Ma magmatic flare-up in the Gangdese belt was most probably related to slab break-off (Fig. 10c) following Neo-Tethyan oceanic slab rollback as suggested by Lee et al. (2009). The detailed evidence is as follows: (1) slab break-off can readily explain the diverse geochemical characteristics of the Linzizong volcanic rocks that likely resulted from multiple magma source regions (e.g., Lee et al., 2012). (2) Geological mapping and geochronological data show that Early Tertiary magmatic rocks crop out in a linear distribution across the southern Lhasa Block. This distribution is consistent with magmatism developed after slab break-off (Chung et al., 2005). (3) Slab break-off can also explain why there was a decrease in the India–Asian convergence rata during the Eocene (Lee and Lawver, 1995) given that break-off would have eliminated slab pull from the existing Neotethyan subduction zone and consequently prevented subduction of the Indian continental lithosphere beneath southern Tibet. (4) Ultrahigh-pressure rock occurrences are consistent with Eocene slab break-off, as has been proposed by previous workers based on Himalayan metamorphic records (Guillot et al., 2003; Kohn and Parkinson, 2002). Leech et al. (2005) suggested that the ~53 Ma ultrahigh-pressure rocks in the NW Himalaya result from early, steep

continental subduction, and proposed that oceanic slab break-off broadly coincided with exhumation of the ultrahigh-pressure rocks in this region. (5) Eocene slab break-off also could explain topographic uplift in southern Tibet (Lee et al., 2009).

6.4. ~30 Ma continental subduction

As mentioned above, the Chongmuda adakitic rocks contain a crustal component from the northward-subducted old Indian continental crust. Moreover, the Chongmuda adakitic rocks have significantly higher La/Yb ratios (47–68) than those (15–36) of the Late Cretaceous crust-derived adakitic rocks (Wen et al., 2008a), indicating that the Chongmuda occurrences may have originated from a deeper crustal source. In addition, Zhang et al. (2010b) suggested that Oligocene (37–32 Ma) high-P (1.8–1.4 GPa) rocks of the High Himalayas and coeval medium-P (0.8–1.1 GPa) rocks of the Lhasa Block represent paired metamorphic belts that resulted from northward subduction of the Indian continent beneath Asia. DeCelles et al. (2011) proposed that the Oligocene–Miocene Kailas basin in southwestern Tibet was likely an extensional feature caused by southward rollback of underthrusting Indian continental lithosphere, following slab breakoff. Therefore, the presence of the ~30 Ma Chongmuda adakitic rocks strongly indicates that the subduction of the Indian continental lithosphere beneath Asia occurred before ca. 30 Ma (Fig. 10d).

7. Conclusions

Sampled Late Cretaceous–Early Oligocene (~91–30 Ma) intrusive rocks in the Chanang–Zedong area correspond to five distinct time periods during the evolution of the GBST, i.e., ~91, ~77, ~62, ~48, and ~30 Ma. Except for the ~77 and ~48 Ma plutons, the other three stages of intrusive rocks are mostly geochemically similar to slab-derived adakites. The ~91 Ma Somka adakitic rocks were derived by partial melting of subducted Neo-Tethyan oceanic crust with minor oceanic sediments. The ~62 Ma Naika and Zedong adakitic rocks were likely generated mainly by partial melting of thickened mafic juvenile lower crust but the source region of the Zedong pluton also contained enriched components from the Indian continental crust. The ~30 Ma Chongmuda adakitic rocks were most probably derived by partial melting of northward subducted Indian lower crust beneath the Lhasa Block. Both the ~77 Ma Luomu diorites and ~48 Ma Lamda granites were likely derived by partial melting of juvenile basaltic lower crust. The tectonodynamic transition from oceanic to continental lithospheric subduction in the GBST took placed between 100 and 30 Ma.

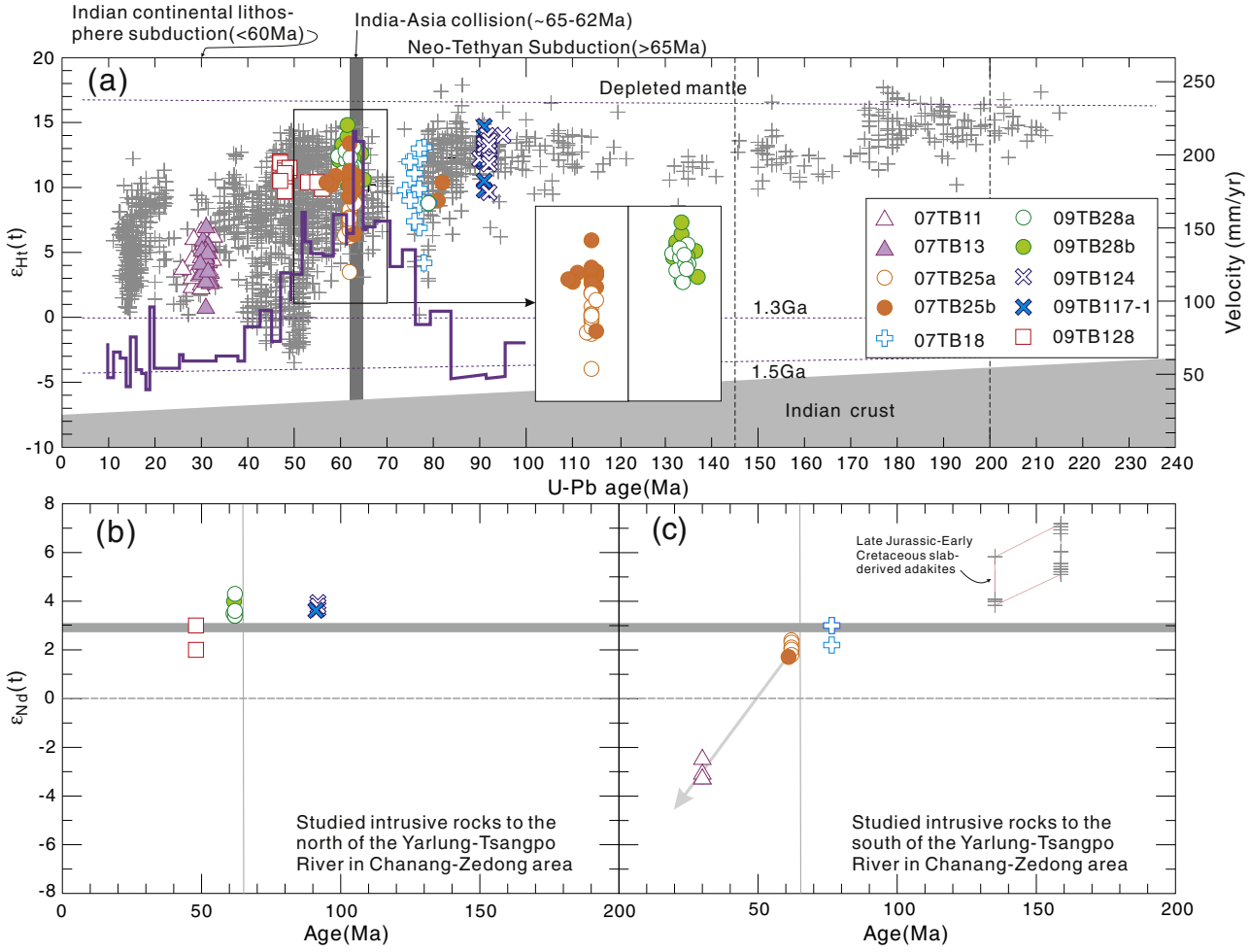

Fig. 9. (a) Plot of $\varepsilon_{Hf}(t)$ versus U–Pb age of zircon from the Gangdese belt. Data are from this study and related literature sources, and correspond to the Triassic–Eocene Gangdese batholith (Chu et al., 2011; Huang et al., 2010; Ji et al., 2009a, 2012; Zhang et al., 2007; Zhu et al., 2011), Late Cretaceous adakites (Guan et al., 2010; Jiang et al., 2012; Zhu et al., 2009), Eo-Miocene adakites (Chung et al., 2009; Guan et al., 2012; Jiang et al., 2011). The data for convergence rate are after White and Lister (2012). (b) Plot of $\varepsilon_{Nd}(t)$ versus zircon U–Pb ages for the intrusive rocks to the northern bank of the Yarlung–Tsangpo River. (c) Plot of $\varepsilon_{Nd}(t)$ versus zircon U–Pb ages for the intrusive rocks to the southern bank of the Yarlung–Tsangpo River. The data for the Late Jurassic–Early Cretaceous slab-derived adakites in (c) are from Wei et al. (2007) and Zhu et al. (2009).

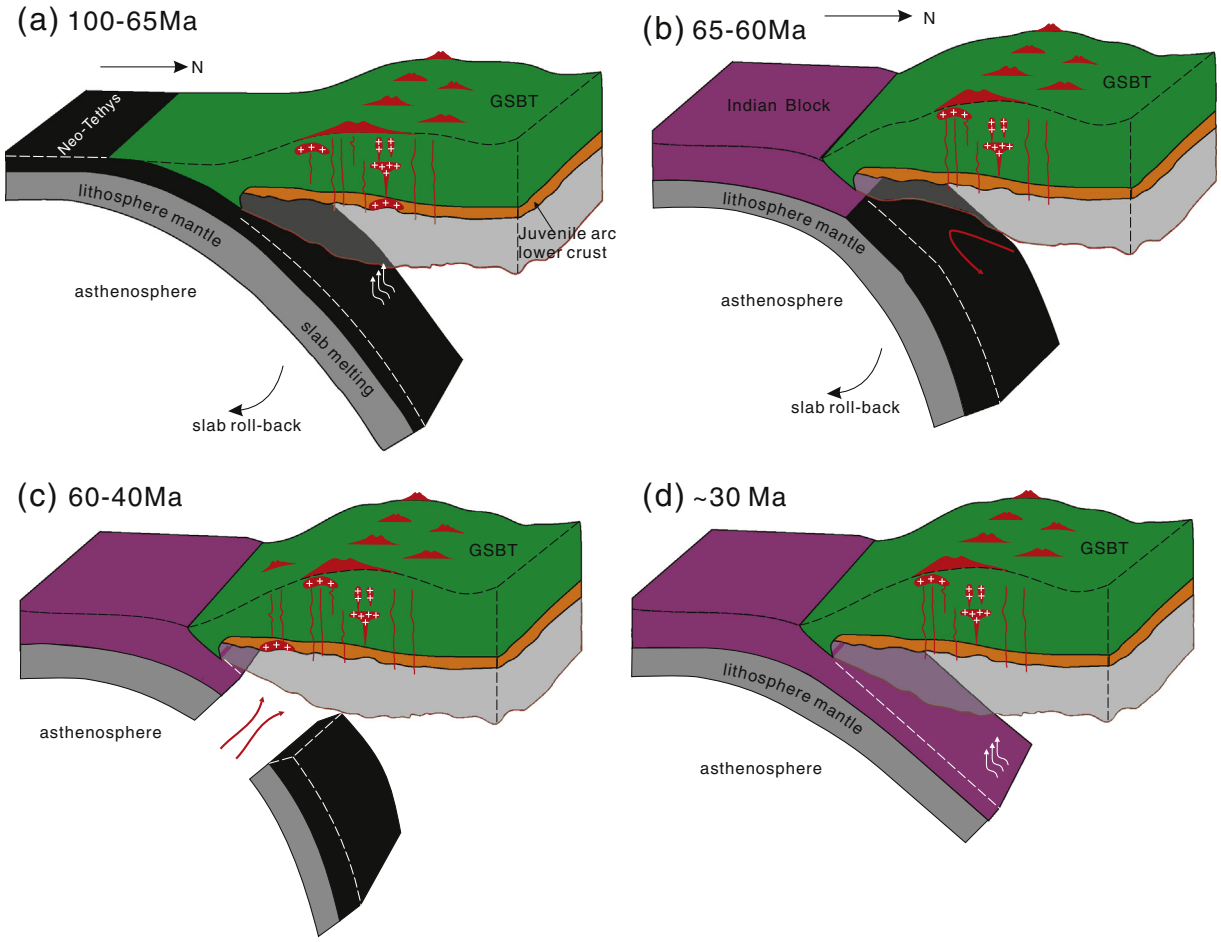

Fig. 10. The suggested model for Late Cretaceous–Oligocene evolution of southern Tibet. (a) 100–65 Ma: rollback of subducted Neo-Tethyan oceanic lithosphere; (b) 65–60 Ma: initial collision between Indian and Asian continents and the crustal thickening of southern Tibet; (c) 60–40 Ma: breakoff of subducted Neo-Tethyan oceanic lithosphere; and (d) ~30 Ma: the northward subduction of the Indian continent.

Supplementary data to this article can be found online at http://dx.doi.org/10.1016/j.lithos.2014.03.001.

Acknowledgments

We sincerely thank Editor-in-Chief Dr. Andrew Kerr, Professor Paul T. Robinson and an anonymous reviewer for their constructive and helpful reviews on this manuscript. We also appreciate the assistance of Hengxiang Yu, Ying Liu, Guangqian Hu, Jinlong Ma, Xirong Liang and Xianglin Tu for their fieldwork and geochemical analyses. This study was jointly supported by the Strategic Priority Research Program (B) of the Chinese Academy of Sciences (grant no. XDB03010600), the National Natural Science Foundation of China (grant nos. 41025006, 41121002 and 41202040) and the Guangzhou Institute of Geochemistry, Chinese Academy of Sciences (GIGCAS 135 project Y234021001). This is contribution No. IS–1851 from GIGCAS, TIGeR publication #503, and contribution 393 from the ARC Centre of Excellence for Core and Crust Fluid Systems (http://www.ccfs.mq.edu.au).

References

Aitchison, J.C., Ali, J.R., Davis, A.M., 2007. When and where did India and Asia collide? Journal of Geophysical Research-Solid Earth 112. http://dx.doi.org/10.1029/2006jb004706.

Aitchison, J.C., Badengzhu, Davis, A.M., Liu, J.B., Luo, H., Malpas, J.G., McDermid, I.R.C., Wu, H.Y., Ziabrev, S.V., Zhou, M.F., 2000. Remnants of a Cretaceous intra-oceanic subduction system within the Yarlung–Zangbo suture (southern Tibet). Earth and Planetary Science Letters 183, 231–244.

Belousova, E.A., Griffin, W.L., O'Reilly, S.Y., Fisher, N.I., 2002. Igneous zircon: trace element composition as an indicator of source rock type. Contributions to Mineralogy and Petrology 143, 602–622.

Cai, F.L., Ding, L., Yue, Y.H., 2011. Provenance analysis of upper Cretaceous strata in the Tethys Himalaya, southern Tibet: implications for timing of India–Asia collision. Earth and Planetary Science Letters 305, 195–206.

Castillo, P.R., Janney, P.E., Solidum, R.U., 1999. Petrology and geochemistry of Camiguin Island, southern Philippines: insights to the source of adakites and other lavas in a complex arc setting. Contributions to Mineralogy and Petrology 134, 33–51.

Castillo, P.R., 2012. Adakite petrogenesis. Lithos 123, 304–316.

Chappell, B., White, A., Wyborn, D., 1987. The importance of residual source material (restite) in granite petrogenesis. Journal of Petrology 28, 1111–1138.

Chu, M.F., Chung, S.L., O'Reilly, S.Y., Pearson, N.J., Wu, F.Y., Li, X.H., Liu, D.Y., Ji, J.Q., Chu, C.H., Lee, H.Y., 2011. India's hidden inputs to Tibetan orogeny revealed by Hf isotopes of Transhimalayan zircons and host rocks. Earth and Planetary Science Letters 307, 479–486.

Chung, S.L., Liu, D.Y., Ji, J.Q., Chu, M.F., Lee, H.Y., Wen, D.J., Lo, C.H., Lee, T.Y., Qian, Q., Zhang, Q., 2003. Adakites from continental collision zones: melting of thickened lower crust beneath southern Tibet. Geology 31, 1021–1024.

Chung, S.L., Chu, M.F., Zhang, Y.Q., Xie, Y.W., Lo, C.H., Lee, T.Y., Lan, C.Y., Li, X.H., Zhang, Q., Wang, Y.Z., 2005. Tibetan tectonic evolution inferred from spatial and temporal variations in post-collisional magmatism. Earth-Science Reviews 68, 173–196.

Chung, S.L., Chu, M.F., Ji, J.Q., O'Reilly, S.Y., Pearson, N.J., Liu, D.Y., Lee, T.Y., Lo, C.H., 2009. The nature and timing of crustal thickening in Southern Tibet: geochemical and zircon Hf isotopic constraints from postcollisional adakites. Tectonophysics 477, 36–48.

Dai, J.G., Wang, C.S., Hébert, R., Santosh, M., Li, Y.L., Xu, J.Y., 2011. Petrology and geochemistry of peridotites in the Zhongba ophiolite, Yarlung Zangbo Suture Zone: implications for the Early Cretaceous intra-oceanic subduction zone within the Neo-Tethys. Chemical Geology 288, 133–148.

DeCelles, P.G., Kapp, P., Quade, J., Gehrels, G.E., 2011. Oligocene–Miocene Kailas basin, southwestern Tibet: record of postcollisional upper-plate extension in the Indus–Yarlung suture zone. Geological Society of America Bulletin 123, 1337–1362.

Defant, M.J., Drummond, M.S., 1990. Oligocene–Miocene Kailas basin, southwestern Tibet: record of postcollisional upper-plate extension in the Indus–Yarlung suture zone. Geological Society of America Bulletin 123, 1337–1362.
Didier, J., Barbarin, B., 1991. Enclaves and Granite Petrology, Developments in Petrology. Elsevier, Amsterdam p625.
Ding, L., Kapp, P., Wan, X.Q., 2005. Paleocene–Eocene record of ophiolite obduction and initial India–Asia collision, south central Tibet. Tectonics 24, 1–18.
Dong, X., Zhang, Z.M., Liu, F., Wang, W., Yu, F., Shen, K., 2011. Zircon U–Pb geochronology of the Nyainqentanglha Group from the Lhasa terrane: new constraints on the Triassic orogeny of the south Tibet. Journal of Asian Earth Sciences 42, 732–739.
Drummond, M.S., Defant, M.J., Kepezhinskas, P.K., 1996. The petrogenesis of slab derived trondhjemite–tonalite–dacite/adakite magmas. Transactions of the Royal Society of Edinburgh: Earth and Environmental Science 87, 205–216.
Escuder, V.J., Contreras, F., Stein, G., Urien, P., Joubert, M., Pérez-Estaún, A., Friedman, R., Ullrich, T., 2007. Magmatic relationships and ages between adakites, magnesian andesites and Nb-enriched basalt-andesites from Hispaniola: record of a major change in the Caribbean island arc magma sources. Lithos 99, 151–177.
Ewart, A., Griffin, W., 1994. Application of proton-microprobe data to trace-element partitioning in volcanic rocks. Chemical Geology 117, 251–284.
Guo, Z.F., Wilson, M., Liu, J.Q., 2007a. Post-collisional adakites in south Tibet: products of partial melting of subduction-modified lower crust. Lithos 96, 205–224.
Gromet, P., Silver, L.T., 1987. REE variations across the Peninsular Ranges batholith: implications for batholithic petrogenesis and crustal growth in magmatic arcs. Journal of Petrology 28, 75–125.
Guan, Q., Zhu, D.C., Zhao, Z.D., Zhang, L.L., Liu, M., Li, X.W., Yu, F., Mo, X.X., 2010. Late Cretaceous adakites in the eastern segment of the Gangdese Belt, southern Tibet: Products of Neo-Tethyan ridge subduction? Acta Petrologica Sinica 26, 2165–2175.
Guan, Q., Zhu, D.C., Zhao, Z.D., Dong, G.C., Zhang, L.L., Li, X.W., Liu, M., Mo, X.X., Liu, Y.S., Yuan, H.L., 2012. Crustal thickening prior to 38 Ma in southern Tibet: evidence from lower crust-derived adakitic magmatism in the Gangdese batholith. Gondwana Research 21, 88–99.
Guillot, S., Garzanti, E., Baratoux, D., Marquer, D., Mahéo, G., de Sigoyer, J., 2003. Reconstructing the total shortening history of the NW Himalaya. Geochemistry, Geophysics, Geosystems 4. http://dx.doi.org/10.1029/2002GC000484.
Guilmette, C., Hebert, R., Wang, C.S., Villeneuve, M., 2009. Geochemistry and geochronology of the metamorphic sole underlying the Xigaze Ophiolite, Yarlung Zangbo Suture Zone, South Tibet. Lithos 112, 149–162.
Guo, F., Nakamuru, E., Fan, W.M., Kobayoshi, K., Li, C.W., 2007b. Generation of Palaeocene adakitic andesites by magma mixing; Yanji area, NE China. Journal of Petrology 48, 661–692.
Guynn, J., Kapp, P., Gehrels, G.E., Ding, L., 2012. U–Pb geochronology of basement rocks in central Tibet and paleogeographic implications. Journal of Asian Earth Sciences 43, 23–50.
Harrison, T.M., Yin, A., Grove, M., Lovera, O.M., Ryerson, F.J., Zhou, X.H., 2000. The Zedong Window: a record of superposed Tertiary convergence in southeastern Tibet. Journal of Geophysical Research-Solid Earth 105, 19211–19230.
Hou, Z.Q., Gao, Y.F., Qu, X.M., Rui, Z.Y., Mo, X.X., 2004. Origin of adakitic intrusives generated during mid-Miocene east–west extension in southern Tibet. Earth and Planetary Science Letters 220, 139–155.
Hou, Z.Q., Zheng, Y.C., Zeng, L.S., Gao, L.E., Huang, K.X., Li, W., Li, Q.Y., Fu, Q., Liang, W., Sun, Q.Z., 2012. Eocene–Oligocene granitoids in southern Tibet: constraints on crustal anatexis and tectonic evolution of the Himalayan orogen. Earth and Planetary Science Letters 349–350, 38–52.
Hu, X.M., Sinclair, H.D., Wang, J.G., Jiang, H.H., Wu, F.Y., 2012. Late Cretaceous–Palaeogene stratigraphic and basin evolution in the Zhepure Mountain of southern Tibet: implications for the timing of India–Asia initial collision. Basin Research 24, 520–543.
Huang, X.L., Xu, Y.G., Lan, J.B., Yang, Q.J., Luo, Z.Y., 2009. Neoproterozoic adakitic rocks from Mopanshan in the western Yangtze Craton: partial melts of a thickened lower crust. Lithos 112, 367–381.
Huang, Y., Zhao, Z.D., Zhang, F.Q., Zhu, D.C., Dong, G.C., Mo, X.X., 2010. Geochemistry and implication of the Gangdese batholiths from Renbu and Lhasa areas in southern Gangdese, Tibet. Acta Petrologica Sinica 26, 3131–3142.
Ingle, S., Weis, D., Doucet, S., Mattielli, N., 2003. Hf isotope constraints on mantle sources and shallow-level contaminants during Kerguelen hot spot activity since 120 Ma. Geochemistry, Geophysics, Geosystems 4. http://dx.doi.org/10.1029/2002GC000482.
Ji, W.Q., Wu, F.Y., Liu, C.Z., Chung, S.L., 2009a. Geochronology and petrogenesis of granitic rocks in Gangdese batholith, southern Tibet. Science in China Series D: Earth Sciences 52, 1240–1261.
Ji, W.Q., Wu, F.Y., Chung, S.L., Li, J.X., Liu, C.Z., 2009b. Zircon U–Pb geochronology and Hf isotopic constraints on petrogenesis of the Gangdese batholith, southern Tibet. Chemical Geology 262, 229–245.
Ji, W.Q., Wu, F.Y., Liu, C.Z., Chung, S.L., 2012. Early Eocene crustal thickening in southern Tibet: new age and geochemical constraints from the Gangdese batholith. Journal of Asian Earth Sciences 53, 82–95.
Jiang, Z.Q., Wang, Q., Wyman, D.A., Tang, G.J., Jia, X.H., Yang, Y.H., Yu, H.X., 2011. Origin of 30 Ma Chongmuda adakitic intrusive rocks in the southern Gangdese region, southern Tibet: partial melting of the northward subducted Indian continent crust? Geochimica 40, 126–146.
Jiang, Z.Q., Wang, Q., Li, Z.X., Wyman, D.A., Tang, G.J., Jia, X.H., Yang, Y.H., 2012. Late Cretaceous (ca. 90 Ma) adakitic intrusive rocks in the Kelu area, Gangdese belt (southern Tibet): slab melting and implications for Cu–Au mineralization. Journal of Asian Earth Sciences 53, 67–81.
Kapp, P., Yin, A., Harrison, T.M., Ding, L., 2005. Cretaceous–Tertiary shortening, basin development, and volcanism in central Tibet. Geological Society of America Bulletin 117, 865–878.
Kapp, P., DeCelles, P.G., Gehrels, G.E., Heizler, M., Ding, L., 2007. Geological records of the Lhasa–Qiangtang and Indo-Asian collisions in the Nima area of central Tibet. Geological Society of America Bulletin 119, 917–933.
Kohn, M.J., Parkinson, C.D., 2002. Petrologic case for Eocene slab breakoff during the Indo-Asian collision. Geology 30, 591–594.
Lee, H.Y., Chung, S.L., Lo, C.H., Ji, J.Q., Lee, T.Y., Qian, Q., Zhang, Q., 2009. Eocene Neotethyan slab breakoff in southern Tibet inferred from the Linzizong volcanic record. Tectonophysics 477, 20–35.
Lee, H.Y., Chung, S.L., Ji, J.Q., Qian, Q., Gallet, S., Lo, C.H., Lee, T.Y., Zhang, Q., 2012. Geochemical and Sr–Nd isotopic constraints on the genesis of the Cenozoic Linzizong volcanic successions, southern Tibet. Journal of Asian Earth Sciences 53, 96–114.
Lee, T.Y., Lawver, L.A., 1995. Cenozoic plate reconstruction of Southeast Asia. Tectonophysics 251, 85–138.
Leech, M.L., Singh, S., Jain, A., Klemperer, S.L., Manickavasagam, R., 2005. The onset of India–Asia continental collision: early, steep subduction required by the timing of UHP metamorphism in the western Himalaya. Earth and Planetary Science Letters 234, 83–97.
Ma, L., Wang, Q., Li, Z.X., Wyman, D.A., Jiang, Z.Q., Yang, J.H., Gou, G.N., Guo, H.F., 2013a. Early Late Cretaceous (ca. 93 Ma) norites and hornblendites in the Milin area, eastern Gangdese: lithosphere–asthenosphere interaction during slab roll-back and an insight into early Late Cretaceous (ca. 100–80 Ma) magmatic "flare-up" in southern Lhasa (Tibet). Lithos 172–173, 17–30.
Ma, L., Wang, Q., Wyman, D.A., Jiang, Z.Q., Yang, J.H., Li, Q.L., Gou, G.N., Guo, H.F., 2013b. Late Cretaceous crustal growth in the Gangdese area, southern Tibet: petrological and Sr–Nd–Hf–O isotopic evidence from Zhengga diorite–gabbro. Chemical Geology 349–350, 54–70.
Ma, L., Wang, Q., Wyman, D.A., Li, Z.X., Jiang, Z.Q., Yang, J.H., Gou, G.N., Guo, H.F., 2013c. Late Cretaceous (100–89 Ma) magnesian charnockites with adakitic affinities in the Milin area, eastern Gangdese: partial melting of subducted oceanic crust and implications for crustal growth in southern Tibet. Lithos 175–176, 315–332.
Macpherson, C.G., Dreher, S.T., Thirlwall, M.F., 2006. Adakites without slab melting: high pressure differentiation of island arc magma, Mindanao, the Philippines. Earth and Planetary Science Letters 243, 581–593.
Mahoney, J.J., Frei, R., Tejada, M.L.G., Mo, X.X., Leat, P.T., NäGler, T.F., 1998. Tracing the Indian Ocean mantle domain through time: isotopic results from old West Indian, East Tethyan, and South Pacific seafloor. Journal of Petrology 39, 1285–1306.
Miller, C., Thöni, M., Frank, W., Schuster, R., Melcher, F., Meisel, T., Zanetti, A., 2003. Geochemistry and tectonomagmatic affinity of the Yungbwa ophiolite, SW Tibet. Lithos 66, 155–172.
McDermid, I.R.C., Aitchison, J.C., Davis, A.M., Harrison, T.M., Grove, M., 2002. The Zedong terrane: a Late Jurassic intra-oceanic magmatic arc within the Yarlung–Tsangpo suture zone, southeastern Tibet. Chemical Geology 187, 267–277.
Middlemost, E.A.K., 1994. Naming materials in the magma/igneous rock system. Earth-Science Reviews 37, 215–224.
Mo, X.X., Hou, Z.Q., Niu, Y.L., Dong, G.C., Qu, X.M., Zhao, Z.D., Yang, Z.M., 2007. Mantle contributions to crustal thickening during continental collision: evidence from Cenozoic igneous rocks in southern Tibet. Lithos 96, 225–242.
Mo, X.X., Niu, Y.L., Dong, G.C., Zhao, Z.D., Hou, Z.Q., Su, Z., Ke, S., 2008. Contribution of syncollisional felsic magmatism to continental crust growth: a case study of the Paleogene Linzizong volcanic Succession in southern Tibet. Chemical Geology 250, 49–67.
Nabelek, J., Hetenyi, G., Vergne, J., Sapkota, S., Kafle, B., Jiang, M., Su, H., Chen, J., Huang, B.S., 2009. Underplating in the Himalaya–Tibet collision zone revealed by the Hi-CLIMB experiment. Science 325, 1371–1374.
Najman, Y., Appel, E., Boudagher-Fadel, M., Bown, P., Carter, A., Garzanti, E., Godin, L., Han, J.T., Liebke, U., Oliver, G., Parrish, R., Vezzoli, G., 2010. Timing of India–Asia collision: geological, biostratigraphic, and palaeomagnetic constraints. Journal of Geophysical Research-Solid Earth 115, B12416. http://dx.doi.org/10.1029/12010JB007673.
Patzelt, A., Li, H.M., Wang, J.D., Appel, E., 1996. Palaeomagnetism of Cretaceous to Tertiary sediments from southern Tibet: evidence for the extent of the northern margin of India prior to the collision with Eurasia. Tectonophysics 259, 259–284.
Peccerillo, A., Taylor, S., 1976. Geochemistry of Eocene calc-alkaline volcanic rocks from the Kastamonu area, northern Turkey. Contributions to Mineralogy and Petrology 58, 63–81.
Rapp, R.P., Watson, E.B., 1995. Dehydration melting of metabasalt at 8–32 kbar: implications for continental growth and crust-mantle recycling. Journal of Petrology 36, 891–931.
Rapp, R.P., Shimizu, N., Norman, M.D., Applegate, G.S., 1999. Reaction between slab-derived melts and peridotite in the mantle wedge: experimental constraints at 3.8 GPa. Chemical Geology 160, 335–356.
Schulte-Pelkum, V., Monsalve, G., Sheehan, A., Pandey, M.R., Sapkota, S., Bilham, R., Wu, F., 2005. Imaging the Indian subcontinent beneath the Himalaya. Nature 435, 1222–1225.
Sen, C., Dunn, T., 1994. Dehydration melting of a basaltic composition amphibolite at 1.5 and 2.0 GPa: implications for the origin of adakites. Contributions to Mineralogy and Petrology 117, 394–409.
Shellnutt, J.G., Jahn, B.M., Dostal, J., 2010. Elemental and Sr–Nd isotope geochemistry of microgranular enclaves from peralkaline A-type granitic plutons of the Emeishan large igneous province, SW China. Lithos 119, 34–46.
Sisson, T., 1994. Hornblende-melt trace-element partitioning measured by ion microprobe. Chemical Geology 117, 331–344.
Streck, M.J.P., Leeman, W., Chesley, J., 2007. High-magnesian andesite from Mount Shasta: a product of magma mixing and contamination, not a primitive mantle melt. Geology 35, 351–354.

Sun, S.S., McDonough, W.F., 1989. Chemical and isotopic systematics of oceanic basalt: implications for mantle compositions and processes. Geological Society of London, Special Publication 42, 313–345.
Sun, Z.M., Pei, J.L., Li, H.B., Xu, W., Jiang, W., Zhu, Z.M., Wang, X.S., Yang, Z.Y., 2012. Palaeomagnetism of late Cretaceous sediments from southern Tibet: evidence for the consistent palaeolatitudes of the southern margin of Eurasia prior to the collision with India. Gondwana Research 21, 53–63.
Tapponnier, P., Zhiqin, X., Roger, F., Meyer, B., Arnaud, N., Wittlinger, G., Jingsui, Y., 2001. Oblique stepwise rise and growth of the Tibet plateau. Science 294, 1671–1677.
van Hinsbergen, D.J.J., Lippert, P.C., Dupont-Nivet, G., McQuarrie, N., Doubrovine, P.V., Spakman, W., Torsvik, T.H., 2012. Greater India Basin hypothesis and a two-stage Cenozoic collision between India and Asia. Proceedings of the National Academy of Sciences 109, 7659–7664.
van Hunen, J., Allen, M.B., 2011. Continental collision and slab break-off: a comparison of 3-D numerical models with observations. Earth and Planetary Science Letters 302, 27–37.
Vervoort, J.D., Patchett, P.J., Blichert-Toft, J., Albarede, F., 1999. Relationships between Lu–Hf and Sm–Nd isotopic systems in the global sedimentary system. Earth and Planetary Science Letters 168, 79–99.
Vervoort, J.D., Patchett, P.J., Albarède, F., Blichert-Toft, J., Rudnick, R., Downes, H., 2000. Hf–Nd isotopic evolution of the lower crust. Earth and Planetary Science Letters 181, 115–129.
Wang, Q., McDermott, F., Xu, J.F., Bellon, H., Zhu, Y.T., 2005. Cenozoic K-rich adakitic volcanic rocks in the Hohxil area, northern Tibet: lower crustal melting in an intracontinental setting. Geology 33 (6), 465–468.
Wang, Q., Wyman, D.A., Xu, J.F., Zhao, Z.H., Jian, P., Xiong, X.L., Bao, Z.W., Li, C.F., Bai, Z.H., 2006a. Petrogenesis of Cretaceous adakitic and shoshonitic igneous rocks in the Luzong area, Anhui Province (eastern China): implications for geodynamics and Cu–Au mineralization. Lithos 89, 424–446.
Wang, Q., Xu, J.F., Jian, P., Bao, Z.W., Zhao, Z.H., Li, C.F., Xiong, X.L., Ma, J.L., 2006b. Petrogenesis of adakitic porphyries in an extensional tectonic setting, Dexing, South China: implications for the genesis of porphyry copper mineralization. Journal of Petrology 47, 119–144.
Wang, Q., Wyman, D.A., Xu, J.F., Wan, Y.S., Li, C.F., Zi, F., Jiang, Z.Q., Qiu, H.N., Chu, Z.Y., Zhao, Z.H., Dong, Y.H., 2008a. Triassic Nb-enriched basalts, magnesian andesites, and adakites of the Qiangtang terrane (Central Tibet): evidence for metasomatism by slab-derived melts in the mantle wedge. Contributions to Mineralogy and Petrology 155, 473–490.
Wang, Q., Wyman, D.A., Xu, J.F., Dong, Y.H., Vasconcelos, P.M., Pearson, N., Wan, Y.S., Dong, H., Li, C.F., Yu, Y.S., Zhu, T.X., Feng, X.T., Zhang, Q.Y., Zi, F., Chu, Z.Y., 2008b. Eocene melting of subducting continental crust and early uplifting of central Tibet: evidence from central-western Qiangtang high-K calc-alkaline andesites, dacites and rhyolites. Earth and Planetary Science Letters 272, 158–171.
Wei, D.L., Xia, B., Zhou, G.Q., Yan, J., Wang, R., Zhong, L.F., 2007. Geochemistry and Sr–Nd isotope characteristics of tonalites in Zetang, Tibet: new evidence for intra-Tethyan subduction. Science in China Series D–Earth Sciences 50, 836–846.
Wen, D.R., Chung, S.L., Song, B., Iizuka, Y., Yang, H.J., Ji, J.Q., Liu, D.Y., Gallet, S., 2008a. Late Cretaceous Gangdese intrusions of adakitic geochemical characteristics, SE Tibet: petrogenesis and tectonic implications. Lithos 105, 1–11.
Wen, D.R., Liu, D.Y., Chung, S.L., Chu, M.F., Ji, J.Q., Zhang, Q., Song, B., Lee, T.Y., Yeh, M.W., Lo, C.H., 2008b. Zircon SHRIMP U–Pb ages of the Gangdese Batholith and implications for Neotethyan subduction in southern Tibet. Chemical Geology 252, 191–201.
White, L.T., Lister, G.S., 2012. The collision of India with Asia. Journal of Geodynamics 56–57, 7–17.
Wu, F.Y., Yang, Y.H., Xie, L.W., Yang, J.H., Xu, P., 2006. Hf isotopic compositions of the standard zircons and baddeleyites used in U-Pb geochronology. Chemical Geology 234, 105–126.
Wu, F.Y., Ji, W.Q., Liu, C.Z., Chung, S.L., 2010. Detrital zircon U–Pb and Hf isotopic data from the Xigaze fore-arc basin: constraints on Transhimalayan magmatic evolution in southern Tibet. Chemical Geology 271, 13–25.
Xiong, X.L., Adam, J., Green, T.H., 2005. Rutile stability and rutile/melt HFSE partitioning during partial melting of hydrous basalt: implications for TTG genesis. Chemical Geology 218, 339–359.
Xu, J.F., Castillo, P.R., 2004. Geochemical and Nd–Pb isotopic characteristics of the Tethyan asthenosphere: implications for the origin of the Indian Ocean mantle domain. Tectonophysics 393, 9–27.
Yang, J.H., Wu, F.Y., Wilde, S.A., Xie, L.W., Yang, Y.H., Liu, X.M., 2007. Tracing magma mixing in granite genesis: in situ U–Pb dating and Hf-isotope analysis of zircons. Contributions to Mineralogy and Petrology 153, 177–190.
Yang, J.S., Xu, Z.Q., Li, Z.L., Xu, X.Z., Li, T.F., Ren, Y.F., Li, H.Q., Chen, S.Y., Robinson, P.T., 2009. Discovery of an eclogite belt in the Lhasa block, Tibet: a new border for Paleo-Tethys? Journal of Asian Earth Sciences 34, 76–89.
Yi, Z.Y., Huang, B.C., Chen, J.S., Chen, L.W., Wang, H.L., 2011. Paleomagnetism of early Paleogene marine sediments in southern Tibet, China: implications to onset of the India–Asia collision and size of Greater India. Earth and Planetary Science Letters 309, 153–165.
Yin, A., Harrison, T.M., 2000. Geologic evolution of the Himalayan–Tibetan orogen. Annual Review of Earth and Planetary Sciences 28, 211–280.
Zeng, L.S., Gao, L.E., Xie, K.J., Liu-Zeng, J., 2011. Mid-Eocene high Sr/Y granites in the Northern Himalayan Gneiss Domes: melting thickened lower continental crust. Earth and Planetary Science Letters 303, 251–266.
Zhang, S.Q., Mahoney, J.J., Mo, X.X., Ghazi, A.M., Milani, L., Crawford, A.J., Guo, T.Y., Zhao, Z. D., 2005. Evidence for a widespread Tethyan upper mantle with Indian-Ocean-type isotopic characteristics. Journal of Petrology 46, 829–858.
Zhang, Z.M., Zhao, G.C., Santosh, M., Wang, J.L., Dong, X., Shen, K., 2010a. Late Cretaceous charnockite with adakitic affinities from the Gangdese batholith, southeastern Tibet: evidence for Neo-Tethyan mid-ocean ridge subduction? Gondwana Research 17, 615–631.
Zhang, Z.M., Zhao, G.C., Santosh, M., Wang, J.L., Dong, X., Liou, J.G., 2010b. Two stages of granulite facies metamorphism in the eastern Himalayan syntaxis, south Tibet: petrology, zircon geochronology and implications for the subduction of Neo-Tethys and the Indian continent beneath Asia. Journal of Metamorphic Geology 28, 719–733.
Zhang, K.J., Zhang, Y.X., Tang, X.C., Xia, B., 2012. Late Mesozoic tectonic evolution and growth of the Tibetan plateau prior to the Indo-Asian collision. Earth-Science Reviews 114, 236–249.
Zhang, Z.M., Dong, X., Xiang, H., Liou, J.G., Santosh, M., 2013. Building of the deep Gangdese arc, south Tibet: Paleocene plutonism and granulite-facies metamorphism. Journal of Petrology 54, 2547–2580.
Zhang, Z.M., Dong, X., Santosh, M., Zhao, G.C., 2014. Metamorphism and tectonic evolution of the Lhasa terrane, Central Tibet. Gondwana Research 25, 170–189.
Zhao, J.H., Zhou, M.F., Yan, D.P., Yang, Y.H., Sun, M., 2008. Zircon Lu–Hf isotopic constraints on Neoproterozoic subduction-related crustal growth along the western margin of the Yangtze Block, South China. Precambrian Research 163, 189–209.
Zhao, J.M., Yuan, X.H., Liu, H.B., Kumar, P., Pei, S.P., Kind, R., Zhang, Z.J., Teng, J., Ding, L., Gao, X., Xu, Q., Wang, W., 2010. The boundary between the Indian and Asian tectonic plates below Tibet. Proceedings of the National Academy of Sciences of the United States of America 107, 11229–11233.
Zhao, Z.D., Mo, X.X., Dilek, Y., Niu, Y.L., DePaolo, D.J., Robinson, P., Zhu, D.C., Sun, C.G., Dong, G.C., Zhou, S., Luo, Z.H., Hou, Z.Q., 2009. Geochemical and Sr–Nd–Pb–O isotopic compositions of the post-collisional ultrapotassic magmatism in SW Tibet: petrogenesis and implications for India intra-continental subduction beneath southern Tibet. Lithos 113, 190–212.
Zheng, Y.C., Hou, Z.Q., Li, W., Liang, W., Huang, K.X., Li, Q.Y., Sun, Q.Z., Fu, Q., Zhang, S., 2012. Petrogenesis and geological implications of the Oligocene Chongmuda–Mingze adakite-like intrusions and their mafic enclaves, southern Tibet. Journal of Geology 120, 647–669.
Zhu, D.C., Zhao, Z.D., Pan, G.T., Lee, H.Y., Kang, Z.Q., Liao, Z.L., Wang, L.Q., Li, G.M., Dong, G.C. , Liu, B., 2009. Early cretaceous subduction-related adakite-like rocks of the Gangdese Belt, southern Tibet: products of slab melting and subsequent melt–peridotite interaction? Journal of Asian Earth Sciences 34, 298–309.
Zhu, D.C., Zhao, Z.D., Niu, Y.L., Mo, X.X., Chung, S.L., Hou, Z.Q., Wang, L.Q., Wu, F.Y., 2011. The Lhasa terrane: record of a microcontinent and its histories of drift and growth. Earth and Planetary Science Letters 301, 241–255.
Zhu, D.C., Zhao, Z.D., Niu, Y.L., Dilek, Y., Hou, Z.Q., Mo, X.X., 2013. The origin and pre-Cenozoic evolution of the Tibetan Plateau. Gondwana Research 23, 1429–1454.